Mechanical behavior of buildings subjected to impulsive motions

Mechanical behavior of buildings subjected to impulsive motions

Mariella Diaferio & Dora Foti*

Department of Civil Engineering and Architecture, Technical University of Bari, Bari, Italy.

*corresponding author, dora.foti@poliba.it

ABSTRACT: This article analyses the response of steel-moment resisting frames subjected to near-field ground motions. In near-field areas high damage and a relevant number of collapsed steel buildings arose even when both design and detailing had been performed in perfect accordance with the code provisions. These circumstances are related to the characteristics of the motion that in such areas shows large-amplitude pulses along the fault-normal component. The response of two steel moment resisting frames characterized by different stiffness levels and subjected to seven different accelerograms recorded in stations located in near-field areas is discussed in the following. The frames have been also analyzed by modelling the real behavior of semi-rigid joints between beams and columns and taking into account the presence of passive dampers (shear link devices). The non-linear dynamic analysis has been performed with the aim of acquiring a quantitative knowledge on the effects of near-field ground motions on frame buildings and on their damage.

Keywords: Near-field motions, Velocity impulse, Semi-rigid nodes, Energy dissipaters.

1. INTRODUCTION

The high number of buildings collapsed or heavily damaged and the high number of victims occurred during the earthquakes of Northridge (1994), Kobe (1995), Kokaeli - Turkey (1999), Chi-Chi Taiwan (1999) and L'Aquila (2009) had a strong impact on the society. In each of these seismic events the hypocenter was located close below the urbanized area, where, however, most victims were recorded. the time histories analysis of the ground motion recorded in areas close to the faults (near-field) during such events, has shown that the characteristics of the component of motion in the direction of rupture propagation of the fault are very different from the usual ones, namely those related to areas far from faults (far-field). In particular, in near-field areas, the component of the ground motion normal to the fault line is impulsive, with a strong short-duration pulse at the beginning of the signal. The above considerations show the necessity to evaluate the behavior of structures subject to near-field earthquakes and to identify possible precautions to be taken in the design phase of these structures in order to reduce their damage. Such damage, in fact, occurred even when the design and detailing of the buildings had been made according to the seismic code requirements. Otherwise, the current seismic standards deal only with problems and calculation procedures related to areas at an intermediate or far distance from faults, for which the characteristics of the ground motion are better known and documented by many and detailed studies present in literature.

These problems can also arise for earthquakes with a low and moderate magnitude. In fact, during an earthquake with a magnitude lower than 6.5 (i.e. San Salvador earthquake in 1986), in near-field regions the recorded damages were similar to those related to major earthquakes (Bommer et al. 2001).

In order to investigate the effects of near-field ground motions, Chopra and Chintanapakdee (2001a) evaluated the elastic and inelastic response spectra of a single degree-of-freedom system subjected to near-field and far-field ground motions. The analysis of the elastic spectra due to near-field earthquakes showed that the maximum values of the velocity spectrum appear in a narrow range of frequencies, while these ranges are wider for both acceleration and displacement spectra.

Chopra and Chintanapakdee (2001b) proposed a displacement spectrum to determine the elastic response of structures to the ground motions in near- and far-field areas. The main aim of this study was to provide important information on the displacements of the ground in near-field areas that cannot be obtained by the seismic codes.

With respect to the time-history plots in near-field areas, the acceleration time-history of the ground shows a pulse in the field of low frequencies and a pronounced pulse in the velocity and displacement time-histories. In this case, the motion is of short duration; on the contrary, in far-field areas, the acceleration, velocity and displacement recordings have the characteristic of a cyclical movement, with a long-lasting action (Mazza and Vulcano 2010; Baker 2007).

Hall (1998) examined the response of six and twenty-storey steel frames subjected to different earthquakes related to near-field seismic zones. In particular, for each of the aforementioned cases two different frames were designed, one in accordance with the UBC 94 standard and the other according to the Japanese standard. The analyzes were performed including the effects of degradation on the welded joints. The low-rise buildings showed the best behavior during strong earthquakes in near-field zones.

Non-linear analyses were also carried out on a six-floor steel frame protected with passive protection systems, friction and viscous ones. the actual behavior of the welded connections between the beam and column was taken into account through the introduction of a constitutive model describing the law of variation of the node stiffness according to the curvature. The analysis showed that both friction and viscous passive control systems are able to significantly reduce the response of such a structure subjected to ground motions in near-field areas. However, these passive protection devices are not able to prevent the failure of the beam-column joints (Filiatrault et al. 2002).

Also for r.c. frames non-linear dynamic analyses put in evidence that, in contrast to what happens in far-field zones, in near-field areas vertical components may be higher than the horizontal ones (Mazza and Mazza 2012; Di Sarno et al. 2011).

In order to identify faster analysis procedures that can be more easily used in engineering practice, Tirca and Gioncu (1998) proposed a modeling of the ground motion in near-field areas. The procedure utilizes artificial accelerograms based on the concept of equivalent velocity pulses. The validity of the proposed procedure was tested by comparing the responses of steel frames subjected to earthquakes related to near-field areas and the equivalent impulses. The results show the complexity of the effects of these actions and the need of an experimental-type research (Alavi and Krawinkler 2004).

Tirca at al. (2003) also examined the response of middle-rise steel frames subjected to near-field earthquakes. It is noted that, as the stiffness of the structure increases, the distribution of the shear forces along the height of the structure presents higher values at higher floors; such behavior is due to the achievement of the yielding stress and the subsequent plastic behavior that is recorded in correspondence of structural elements arranged on the upper floors. It must be also underlined that for frames of reduced stiffness, the maximum ductility demand migrates from the top towards the base of the building. Therefore, to significantly reduce the ductility demand and avoid the collapse of the structure, the strength of the upper part of the slender frames must be increased, i.e. keeping the cross section of the column constant along the total height.

This new aspect was emphasized in the study of the response of frames with friction dampers and subjected to the signals of a same earthquake recorded both in far-field areas and in near-field ones (Foti 2014a). A frame without any protection device absorbs most of the input energy and, consequently, is subjected to strong accelerations and large interstorey drifts. On the contrary, a frame protected with friction dissipaters shows the development of plastic hinges at the beam-column joints, while the plastic deformations are mainly concentrated in the dissipaters, which can be easily replaced after an earthquake. Although passive dissipation systems are able to significantly reduce the response of the frame structures subjected to near-field motions, they cannot prevent the collapse. However, these systems can be used to avoid the development of collapse mechanisms of the floor. Nevertheless, in some cases the interstorey drift does not satisfy the code requirements. The latter circumstance suggests the adoption of design criteria specifically developed for structures in near-field areas.

The same kind of frames were analyzed when equipped with dissipaters or isolators. Their responses due to near-field ground motions was compared (Foti 2014b). On the basis of the results obtained in terms of shear forces, interstorey drifts, ductility capacity and damage indexes, it is possible to notice a better behavior of the frame equipped with dissipaters respect to the base isolated one.

The effect of the local soil was also considered (Foti 2015) and the response was compared with multi-floor frames equipped with two kinds of dissipaters - hysteretic and friction dissipaters - highlighting the differences for the two cases.

The present article deals with the response of two six-story steel buildings having different stiffness characteristics and subjected to seven near-field earthquake records. The frames have been designed according to the prescription of Eurocodes 3 and 8 (EN-1998 2004; EN-1998 2003). The beam-column joints were modeled as semi-rigid nodes. The main aim of the study is to analyze the response of such structures also when they are equipped with passive dissipaters. In the latter case it has been chosen to install shear link devices whose behavior is mostly conditioned by their shear deformations.

In literature a lot of dissipaters characterized by a shear behavior have been proposed: dissipaters made by steel (Chais et al. 1997; Chais et al. 2000, Chais et al. 2001, Ponzo 2012), other realized combining aluminum and steel (Foti et al. 2010; Foti et al. 2013). They are able to reduce the interstorey drifts that activate the dissipation in the device. In the present study it has been chosen to adopt the Shear Link device (SL) which is a steel dissipater with a hysteretic dissipative behavior (Chais et al. 1997; Chais et al. 2000; Chais et al. 2001).

We analyzed the response of the frames, with and without hysteretic dissipaters, induced by seven near-field earthquake records, with the aim of determining the behavior of the protected structures varying the stiffness characteristics of the frame.

The response of the examined frames is described in terms of damage indices, base shear, interstorey drifts and acceleration amplification

2. FRAME STRUCTURES

2.1 Geometric Characteristics

Two steel six-floor frames have been considered, called MRF1 and MRF2; each of them has a total height of 19 m and two equal 6 m spans (Figure 1).

All beams are realized with IPE 360 profiles, while the columns are made with HEB profiles. The cross section of the columns varies in correspondence of the third floor (Figure 1). The difference between the two frames is related to the dimensions of the profile of the columns (see Table 1). In detail, MRF2 frame is stiffer than MRF1 as it is possible to noticed from the first fundamental periods of the unprotected frames. The difference between the two frames is related to the dimensions of the profile of the columns, as it is shown in Table 1. In detail, MRF2 frame is characterized by a higher stiffness.

The frames have been considered subjected to structural self- weights and to a load of 20000 N uniformly distributed on each beam.

According to the current Italian code (NTC08), it has been assumed that the site is characterized by a PGA at the bedrock with a 475 years return period equal to a_g = 0.233 g. For the site effect an amplification factor S = 1.377 has been considered, corresponding to a deposits with predominant soft-to-medium stiff cohesive soils.

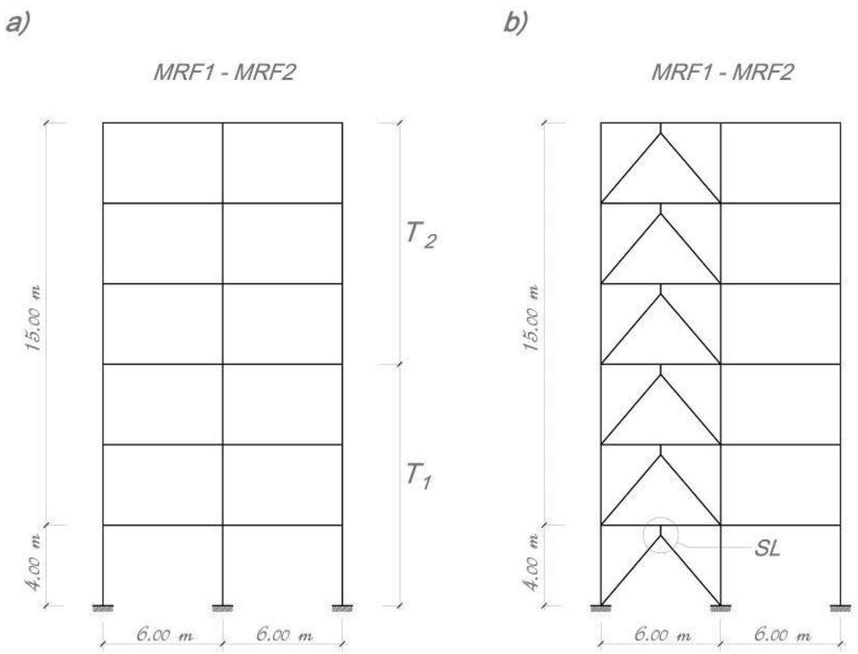

Figure 1. Geometric characteristics of MRF1 and MRF2 frames a) without protection; b) protected with SL devices.

Table 1 shows the characteristics of the cross sections of the columns of the frames and the periods of the first three natural modes referred to the unprotected (bare) frame.

Table 1. Geometrical characteristics and natural periods of MRF1 and MRF2 frames.

Frame	Columns				Beams		Period [s]		
	T1		T2		T1	T2	T_{s1}	T_{s2}	T_{s3}
	Lateral	Central	Lateral	Central					
MRF1	HE200B	HE240B	HE160B	HE180B	IPE360	IPE360	1.53	0.55	0.32
MRF2	HE450B	HE500B	HE400B	HE450B	IPE360	IPE360	0.88	0.25	0.12

2.2 Semi-rigid nodes

For a more accurate assessment of the global behavior and strength capacity of the connections in steel structures, the beam-column joints were modeled as semi-rigid nodes. This modeling is important in cases when it is necessary to accurately assess the effects of local deformations developed within the links as a consequence of the bending and shear forces. These effects, in fact, can have a considerable influence on the distribution of internal forces in structural elements, on the stability of the members and on the displacements of the structure due to vertical and horizontal loads. It is important, therefore, to evaluate these effects by introducing a more accurate model of the behavior of such joints. The use of semi-rigid joints has the advantage of reducing the construction costs. Compared to the rigid joints, in fact, the semi-rigid ones usually allow to simplify the constructive details and to obtain a reduction of the cost of workshop and assembly. The latter compensate a possible increment of the dimensions of some structural elements.

In this paper, in order to describe the behavior of semi-rigid nodes, in the finite element models of the structures we have introduced a nonlinear link with a moment-curvature law defined on the basis of the results of experimental investigations and analytical processing (SPRINT RA351 1995). The aforementioned study takes into account the semi-rigid joints subjected to a moment. Specifically, the deformations due to the bending of the joint and to the shear deformation of the column web are evaluated to define the moment-curvature law for different combinations of the dimensions of beam and column cross-sections and of the details of the connection.

As a result of the above deformations of the node, the relative rotation θ at the end of the geometric axis of the beam with respect to the geometric axis of the column (Figure 2a) can be evaluated; in Figure 2b the bending moment-rotation (M-θ) law is plotted. In particular, it can be observed that when the moment increases, a partial plasticization of the connection occurs, which is associated with a gradual reduction of the initial stiffness K_1 of the node (see the second branch of the curve in Figure 2b). In the case here considered, the beam-column connections of the frames were realized using a flanged solution with 8.8 and 16 mm diameter bolts. Table 2 shows the mechanical properties of these semi-rigid nodes for MRF1 and MRF2 frames.

a) b)

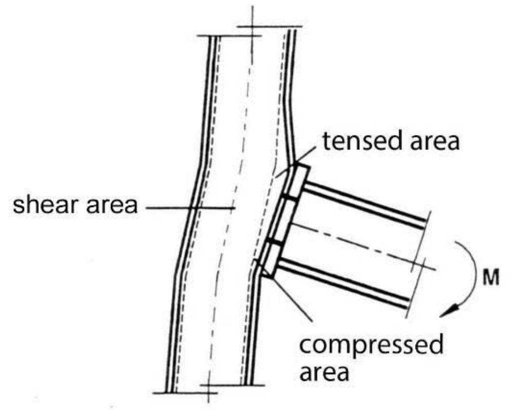

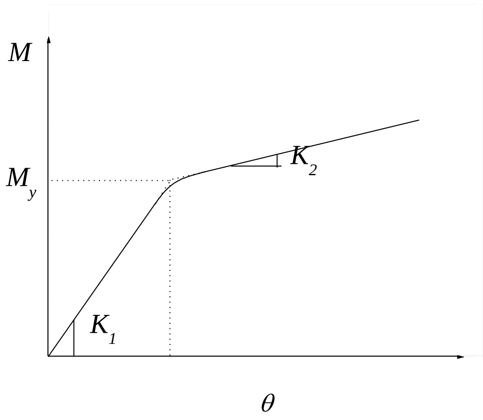

Figure 2. a) Deformation of a beam-column joint (SPRINT RA351 1995); b) Constitutive behavior of a beam-column semi-rigid node.

Table 2. Mechanical characteristics of semi-rigid nodes for MRF1 and MRF2 frames.

Column	**Beam**	**K_1 [KN m/rad]**	**M_y [KN m]**	**K_2/ K_1**
HEB 160	IPE 360	16199	24.9	0.2491
HEB 180	IPE 360	20854	30.1	0.2494
HEB 200	IPE 360	23012	79.2	0.2506
HEB 240	IPE 360	24783	32.5	0.2534
HEB 500	IPE 360	24119	32.5	0.2501
HEB 550	IPE 360	23368	32.5	0.2501
HEB 600	IPE 360	22670	32.5	0.2502

3. HYSTERETIC DAMPERS FOR THE SEISMIC PROTECTION

3.1 Shear-Link Device

The aforementioned frames were protected by means of passive dampers called "Shear-Link" (SL) (Chais et al. 1997; Chais et al. 2000; Chais et al. 2001). They were installed in the structure at the intersection of two diagonals (made with 200x200x1.2 mm square section tubes) and the upper beam (Figure 1b). SL devices are made in mild steel and are characterized by a rectangular shape along the longitudinal direction and by a "double-T" shaped cross section. In order to avoid buckling phenomena, the steel plate, that is the main part of the device, is equipped with transversal and longitudinal stiffeners that subdivided the steel plate in five rectangular plates, as shown in Figure 3. The total height of the device is approximately 25.4 cm plus 2.5 cm for the plates that connect the device to the surrounding frame elements (diagonals and beam).

An important characteristic of the dissipater is that the size can be easily varied in order to obtain different yielding forces, i.e. the force for the activation of energy dissipation (Chais et al. 1997; Chais et al. 2000; Chais et al. 2001). Such devices allow to dissipate energy through the plastic deformation of the mild steel of the web plate, this deformation being mainly due to the shear stresses. The device is characterized by stable hysteresis curves under cycles of loading and unloading. The geometry of an SL device allows a uniform dissipation throughout the central area, avoiding the occurrence of local stress concentrations that could reduce the dissipation capability (Figure 4).

The dissipater is very stiff in the cross section, that is the plane in which the shear forces due to the seismic load act, and flexible in the plane orthogonal to the plane of the frame. In order to reduce such flexibility the shape of the device presents the above described stiffeners in this direction that have the aim of reducing the possibility of an out-of-plane instability of the device. The chosen shape has the advantage of allowing to dissipate energy for very small deformations and, therefore, for interstorey drifts smaller than those commonly considered for other types of hysteretic dampers.

a) **b)**

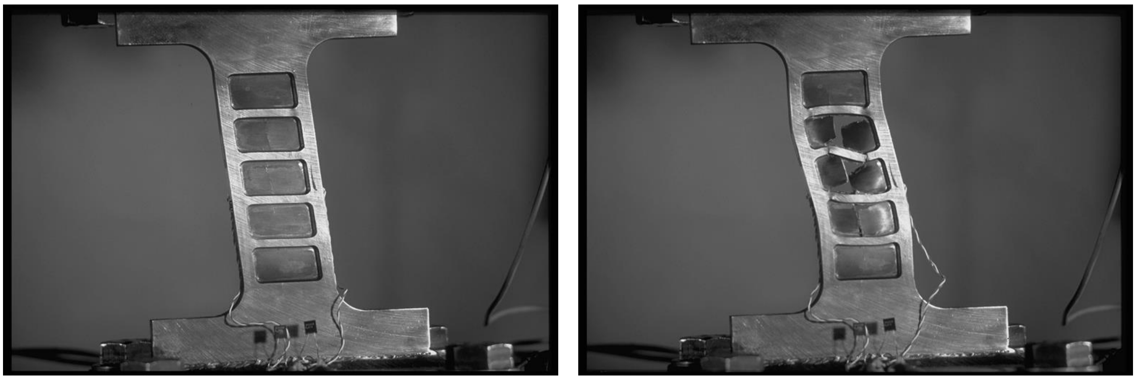

Figure 3. Shear-Link (SL) device. a) shear behavior; b) bending behavior (Chais et al. 2001).

It can be observed that, after the failure of the thinner parts, the device shows additional strength reserves. It can still support increment of loads but its behavior changes from a shear-type behavior to a bending-type one (Figure 4). On the basis of such characteristics SL device has been chosen to evaluate its efficacy in the protection of steel frames subject to near-field motions. The finite element model of the device has been defined in accordance with the results of the characterization tests.

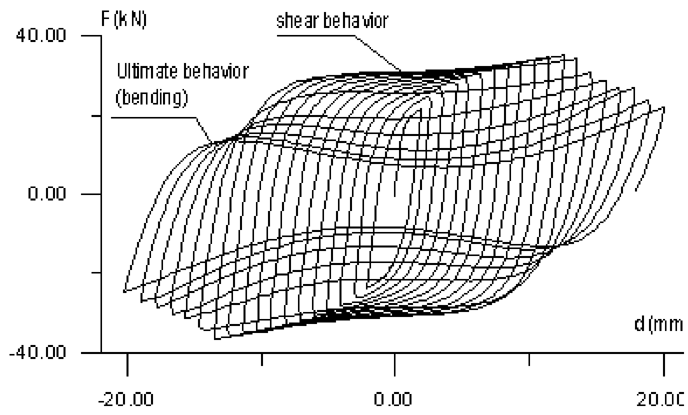

Figure 4. Hysteretic curve for SL device obtained by characterization tests (Chais et al. 2000; Chais et al. 2001).

3.2 Design criterion of SL device

SL devices have been installed in the protected frames in correspondence of each floor by introducing two diagonals (as described in section 3.1).

As a first step the yielding forces of SL devices have been evaluated analyzing the two frames equipped at each floor with two diagonals, realized with 200x200x1.2 mm square tubes. These diagonals have been arranged similarly to what shown in Figure 1b, except for the absence of an SL device. In detail, the two diagonals have been considered directly connected to the beam positioned at the upper floor. These frames have been subjected to equivalent static horizontal forces evaluated according to the Italian seismic code (NTC 2008) for an area of high seismic risk. The size of the SL device at each floor of the frame has been designed imposing that the yielding force (i.e. the shear force at the beginning of the plastic behavior of the device) is equal to the 75% of the horizontal component of the resultant forces in the diagonals positioned at the considered level and evaluated as previously explained.

4. NEAR-FIELD GROUND MOTIONS

The analysis of the time histories of near-field ground motions shows that, when the fracture generated by the seismic shock propagates with a speed close to the shear waves, most of the energy released during the earthquake produces a pulse of high intensity at the beginning of the phenomenon. This pulse is recorded in the component of motion along the direction perpendicular to the fault line. Consequently, the motion that develops in this direction is characterized by pulses of great amplitude in the velocity and in the displacement time histories, while the motion recorded in the opposite direction of the propagation of the fault does not show pulse characteristics.

In addition, the velocity peak of the component of motion in the direction of propagation of the fault is even three times larger than the one of the component of motion in the opposite direction; also, the values of acceleration and displacement are higher.

A nonlinear dynamic analysis of the frames has been performed taking into account the following seven near-field earthquakes:

- Duzce-Turchia, November 1999; two accelerograms recorded, respectively, in Duzce and in Bolu;
- Kobe, 1995; two accelerograms recorded, respectively, in Kobe-JMA and Takatori;
- Northridge 1994; two accelerograms recorded, respectively, in Rinaldi and Sylmar;
- Kokaeli, August 1999, recorded in Yarimka.

The characteristics of the seven near-field ground motions are summarized in Table 3.

Table 3. The seven near- field ground motions considered for the analysis.

Simbol	Earthquake (epicentre and date)	Station	Component	Magnitude	Distance (Km)	PGA (cm/s^2)
KobeJMA	KOBE ‘95	KOBE-JMA	90°	6.9	0.6	599
Kobe90	KOBE ‘95	Takatori	90°	6.9	0.3	616
Sylma228	Northridge ‘94	Rinaldi	228°	6.7	7.1	838
Sylma52	Northridge ‘94	Sylmar	52°	6.7	6.2	612
Kokaeli60	Kokaeli 08.’99	Yarimca	60°	7.4	2.6	268
Duzce270	Duzce 11.09	Duzce	270°	7.1	8.2	535
Duzce90	Duzce 11.09	Bolu	90°	7.1	17.6	822

In Figure 5 the response spectra of the seven earthquake records are shown for a damping coefficient equal to 5%.

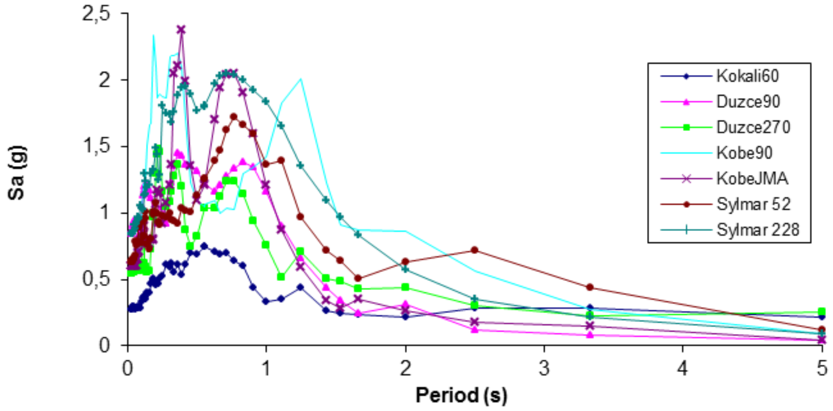

Figure 5. Response spectra of the seven near-field ground motions (see Table 3).

5. DYNAMIC ANALYSIS RESULTS

Figures 6 and 7 show the maximum interstorey drift, δmax, expressed as a percentage of the storey height h plotted for each signal. This parameter is indicative of both structural and non-structural damages; the seismic codes imposes a limit to its maximum value. In particular, EC8 (EN-1998 2003) imposes that δmax does not exceed 0.01 h, while ACI 318-14 (ACI committee 318 2014) prescribes $\delta max /h$ = 0.2% for the serviceability limit state and $\delta max / h$ = 1.5% for the ultimate limit state.

The results of the nonlinear dynamic analysis show that the unprotected frames (Figures 6a and 7a), for all the considered earthquakes, suffer interstorey drifts significantly higher than those allowed by EC8 (up to 6 times higher); such drifts are also 5 to 20 times higher than those acceptable by ACI for the serviceability limit state and, furthermore, do not respect the limit set for the ultimate limit state, except for Kokaeli60 record.

Figure 6a shows that for MRF1 bare frame the highest values of the interstorey drifts are achieved in correspondence of the 4^{th} level. This behavior is particularly noticeable for Sylmar 228, Sylmar 52 and Kobe90 earthquakes (see Table 3), and it is due to the contribution of the higher vibration modes to the structural response.

The behavior described above is considerably modified by the introduction of shear links, which allow to reduce the interstorey drifts about four times those of the bare frame (Figure 6b). The introduction of dissipaters, in addition, significantly alters the trend of such drifts along the height of the frame that, in this case, is almost constant, differently from the bare frame (Figure 6a). Moreover, the response of the protected frame shows that the presence of shear links produces the highest effects at the top levels. In detail, the interstorey drifts, except for Kobe JMA and Sylmar 228 records, achieve values lower than 1% of the storey height, as requested by EC8.

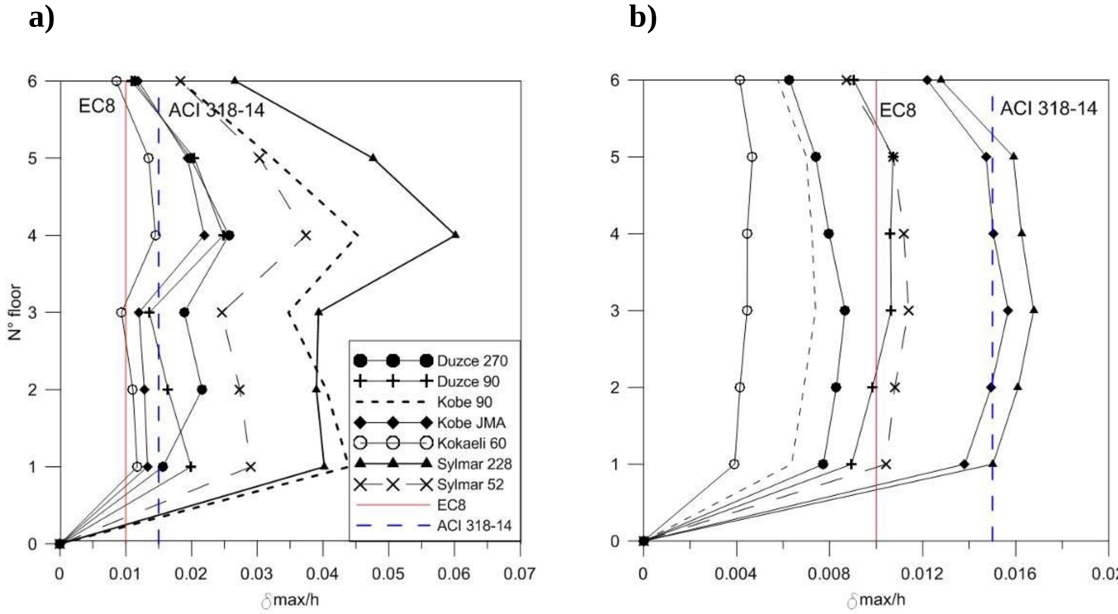

Figure 6. Interstorey drifts for MRF1 frame (Table 1). a) Bare frame; b) frame with semi-rigid joints and shear links.

In the case of the bare frame, when the stiffness of the frame increases (MRF2 frame), the variation of the interstorey drifts along the height of the frame changes. More specifically, there is a migration of the peak values of these drifts towards lower floors and a less variability along the height of the building (Figure 7a).

Moreover, the amplitude of these drifts is about a half of those obtained for MRF1 frame. However, except for Kokaeli 60 (see Table 3), for all the examined earthquakes the requirements of both EC8 and ACI are not fulfilled.

a) **b)**

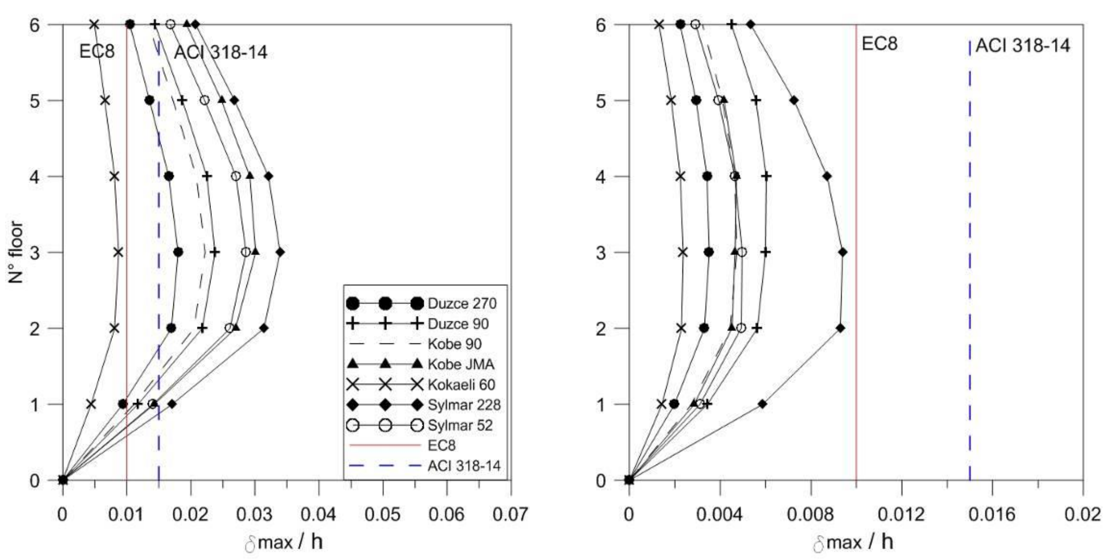

Figure 7. Interstorey drifts for MRF2 frame (Table 1). a) Bare frame; b) frame with semi-rigid joints and shear links.

Similarly to MRF1 frame, the protected MRF2 frame shows a significant reduction of the interstorey drifts, which, in fact, for all the considered earthquake signals assume values compatible with the limits imposed by EC8. The beneficial effect obtained by the introduction of shear links, however, is also confirmed by analyzing the damage index (i.e. the ratio between the maximum displacement, *Dmax* and the total frame height, *H*) that, in fact, shows a considerable reduction compared with the bare frame (Figure 8a).

MRF2 frame presents a reduction of the damage index greater than MRF1 frame (Figure 8b).

a) **b)**

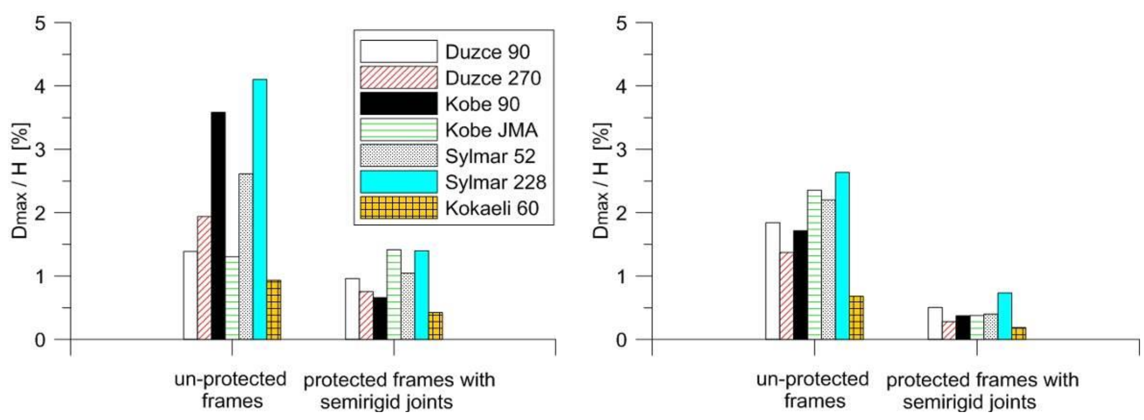

Figure 8. Damage index [*Dmax/H* %]. a) Bare and protected MRF1 frames; b) bare and protected MRF2 frames.

Figure 9 shows, for all the examined earthquakes, the shear forces *V* at the base of the columns, expressed as a ratio of the total weight *W* of the frame. The comparison between the values of the shear forces for the two investigated bare frames shows, as expected, a significant increase of these values as the stiffness of the frame increases.

Figure 9 highlights that the introduction of shear links causes a significant reduction of the shear forces in the columns, that is more pronounced in the case of MRF2 frame, with clear benefits for the structure.

Moreover, for MRF1 frame, the maximum reduction of the shear forces with respect to the bare frame is achieved for Kobe90 earthquake (reduction of 85.52 %), while for Kobe–JMA earthquake the shear forces slightly increases if compared to the bare frame (up to 2.8 %).

MRF2 frame, however, exhibits a uniform reduction of the shear forces for all the examined near-field motions (Figure 9b).

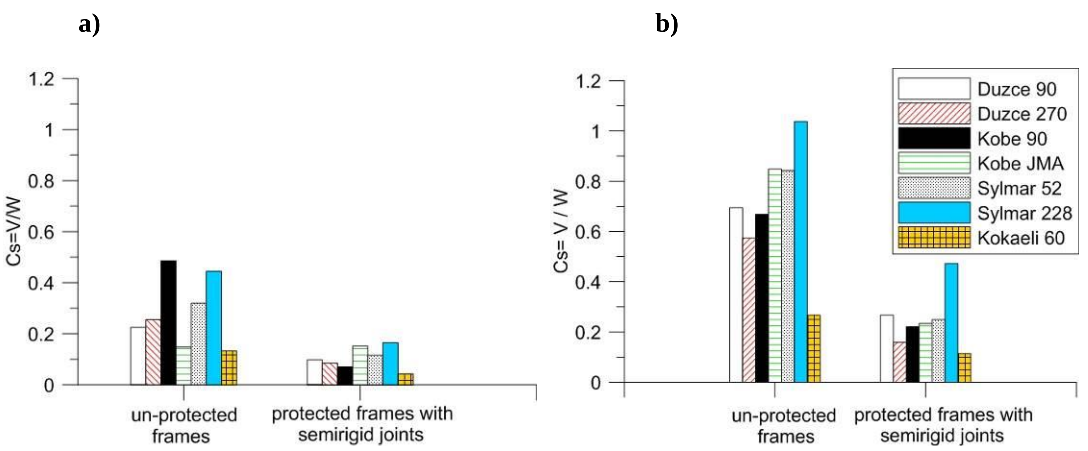

Figure 9. Ratio between the shear forces *V* at the base of the columns, and the total weight of the frame (*Cs= V/W*). a) Bare and protected MRF1 frames; b) bare and protected MRF2 frames.

Figure 10 shows the acceleration amplification at each floor for both un-protected and protected MRF2 frames. The latter case is referred to frames with semi-rigid joints. Figure 10 highlights that in the case of bare frame Sylmar 228 and Kokaeli 60 induce the highest values of the acceleration amplification at almost all the floors. The frame protected with Shear Links shows an increase of the accelerations mainly due to the presence of the diagonals, which increase the total stiffness of the frame. This result is due to the shift of the fundamental period towards values close to the "plateau" of the spectra. However, the increment is not so relevant and evidences a good design of the dissipation system. As a consequence, the increment of the stiffness is partly compensated by a uniform reduction of the spectra due to the dissipation effects, at least for some of the near-field signals utilized in the analysis. Foti (2014b) found the same results comparing the acceleration amplifications of a frame without diagonals and with Shear Link dissipative devices.

a)

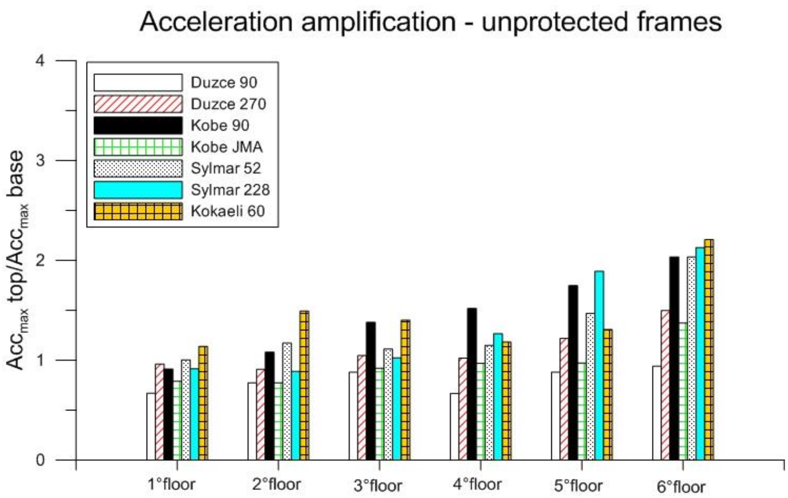

b)

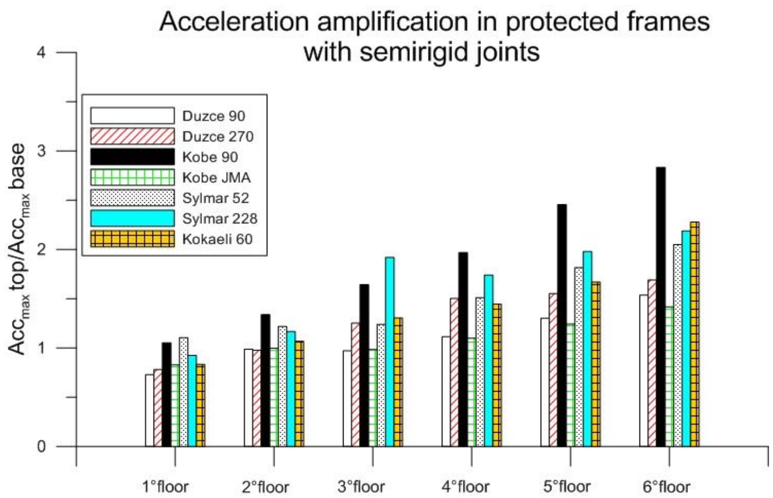

Figure 10. Acceleration amplification at each floor of MRF2 frame for a) unprotected frames and b) protected frames with semi-rigid joints.

Figure 10b displays a decisive increment of the acceleration for Kobe 90, especially from the 4th floor. The protected frame shows for the Kokaeli 60 a reduction of the acceleration amplification, especially at the lower floors.

Figure 11 shows the hysteretic loop of the Shear Link installed at the 4th floor of MRF1 frame evaluated for Kobe-JMA earthquake. It can be observed that the dissipater undergoes a large hysteretic loop producing, therefore, a high energy dissipation. The same behavior has been observed also for all the other examined near-field motions.

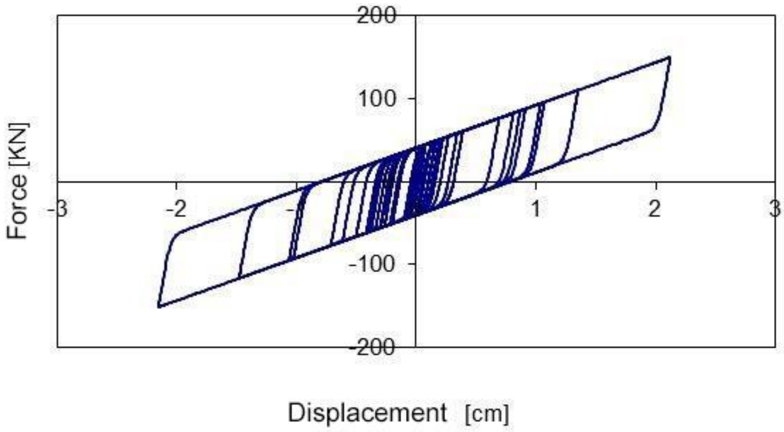

Figure 11. Hysteresis loop of the Shear Link installed at the 4th floor of MRF1 frame subjected to Kobe-JMA earthquake.

6. CONCLUSIONS

The present paper investigates the behavior of two steel frames with different stiffness characteristics and subjected to seven near-field ground motions. The nonlinear dynamic analysis was conducted following two hypotheses: 1) the beam-column joints are rigid nodes; 2) the beam-column joints are semi-rigid nodes and at each floor a passive protection device of the Shear Link-type is installed. In detail, the Shear Links have been dimensioned in order to undergo plastic deformations for a shear force equal to a prescribed percentage of the maximum floor shear force evaluated on the bare frame.

The analysis has been performed in terms of interstorey drifts, damage index, shear forces and acceleration amplifications at the base of the frames. The comparison of the responses of the two frames with and without Shear Links shows that the introduction of these devices allows a significant improvement of the behavior of the frames, particularly evident for the one characterized by a higher stiffness. In the latter case, in fact, it is possible to obtain values of the interstorey drifts compatible with the limits set by the seismic codes.

The benefits of the presence of Shear Links were also observed with respect to the damage index and the shear forces at the base of the columns.

The present study allows to underline possible suggestions for the seismic retrofitting of existing buildings. An example is the possible analysis of the advantages originated from interventions that provide the introduction of Shear Links and an increase of the stiffness of the frame. For all the examined near-field motions, in fact, the dynamic analysis shows that the efficacy of the Shear Links increases with the stiffness of the frame.

REFERENCES

ACI committee 318, (2014). *ACI 318-14: Building Code Requirements for Structural Concrete and Commentary*, 0-520. ISBN: 9780870319303.

Alavi B, Krawinkler H (2004) Behavior of moment-resisting frame structures subjected to near-fault ground motions. Earthq Eng and Struct Dyn. 33(6):687-706.

Baker JW (2007) Quantitative classification of near-fault ground motions using wavelet analysis. Bull of the Seismol Soc of America. 97(5):1486-1501.

Bommer J, Georgallides G, Tromans IJ (2001) Is there a near-field for small-to-moderate magnitude earthquakes?. J of Earthq Eng 5(3):395-423.

Chais X, Bozzo LM, Torres L, Foti D (1997) An Energy Dissipating Devices for Seismic Protection of Masonry. Proc of the “8° Convegno Nazionale L’Ingegneria Sismica in Italia, Taormina, 21-24 September, p.1005-1011.

Chais X, Torres L, Bozzo L (2000) An innovative elasto-plastic energy dissipater for the structural and non-structural building protection Proc of the 12th World Conference on Earthquake Engineering; Auckland, New Zeland, 30 January - 4 February.

Chais X, Bozzo L, Torres L, Foti D (2001) Experimental Tests on Hybrid,Semi-active and Passive Devices for Seismic Risk Mitigation. In: Report n°7, ISMES, Ed. Giorgio Franchioni Rew. R.T. Severn, C. Taylor, Part 2.

Chopra AK and Chintanapakdee C (2001a) Comparing response of SDF systems to near-fault and far-fault earthquake motions in the context of spectral regions. Earthq Eng and Struct Dyn 30:1769-1789.

Chopra AK and Chintanapakdee C, (2001b) Drift Spectrum vs. Modal Analysis of Structural Response to Near-Fault Ground Motions. Earthq Spectra 17(2):221-234.

Di Sarno L, Elnashai AS, Manfredi G (2011) Assessment of RC columns subjected to horizontal and vertical ground motions recorded during the 2009 L'Aquila (Italy) earthquake. Eng Struct 33(5):1514-1535.

EN-1998. (2003) Eurocode 8:design of structures for earthquake resistance – Part1: general rules, seismic actions and rules for buildings. C.E.N., European Committee for Standardisation.

EN-1998 (2004). Eurocode 3:design of steel structures – Part1: general rules and rules for buildings. C.E.N., European Committee for Standardisation.

EN-1998 (2004). Eurocode 3:design of steel structures – Part1: general rules and rules for buildings. C.E.N., European Committee for Standardisation.

Filiatrault A, Tremblay R, Wanitkorkul A (2002) Performance Evaluation of passive damping systems for the seismic retrofit of steel moment-resisting frames subjected to near-field ground motions. Earthq Spectra 17(3):427-437.

Foti D (2014a) On the seismic response of protected and unprotected middle-rise steel frames in far-field and near-field areas. Shock and Vibration. Article ID 393870, ISSN: 10709622, doi: http://dx.doi.org/10.1155/2014/393870.

Foti D (2014b) Response of frames seismically protected with passive systems in near-field areas. Int J of Structural Eng 5(4):326-345.
Doi: http://www.inderscience.com/info/ingeneral/forthcoming.php?jcode=ijstructe

Foti D (2015) Local ground effects in near-field and far-field areas on seismically protected buildings. Soil Dyn and Earthq Eng 74:14-24, doi: http://dx.doi.org/10.1016/j.soildyn.2015.03.005

Foti D, Diaferio M, Nobile R (2010) Optimal design of a new seismic passive protection device made in aluminium and steel. Struct Eng and Mech 35(1):119-122.

Foti D, Diaferio M, Nobile R (2013) Dynamic behavior of new aluminum-steel energy dissipating devices. Struct Control and Health Monitoring 20(7):1106-1119.

Hall JF (1998) Seismic response of steel frame buildings to near-source ground motions. Earthq Eng and Struct Dyn 27:1445-1464.

Mazza F, Mazza M. (2012) Nonlinear modeling and analysis of r.c. framed buildings located in near-fault areas. Open Construction and Building Technology J 6:346-354.

Mazza F, Vulcano A (2010) Nonlinear dynamic response of r.c. framed structures subjected to near-fault ground motions. Bull of Earthq Eng 8(6):1331–1350.

Norme Tecniche per le Costruzioni (NTC) (2008). 'Italian Ministry of Infrastructures', Nuove norme tecniche per le costruzioni e relative istruzioni, D.M.14-01-2008 e Circolare 02-02-2009, n. 617/C.S.LL.PP.

Ponzo FC, Di Cesare A, Nigro D, Vulcano A, Mazza F, Dolce M, Moroni C (2012) Jet-pacs project: Dynamic experimental tests and numerical results obtained for a steel frame equipped with hysteretic damped chevron braces. J of earthq Eng 16(5):662-685.

SPRINT RA351 bis Contract (1995) Final Report. Semi-rigid joints in steel constructions. A simple calculus procedure and the design tables.

Tirca L, Gioncu V (1998) The effects of horizontal and vertical ground motion near and far field regions. Proc. of the "2nd Int. Ph.D. Symposium in Civil Engineering", Budapest: 461-468.

Tirca L, Foti D, Diaferio M (2003) Response of middle-rise steel frames with and without passive dampers to near-field ground motions. Eng Struct 25(2):169-179.

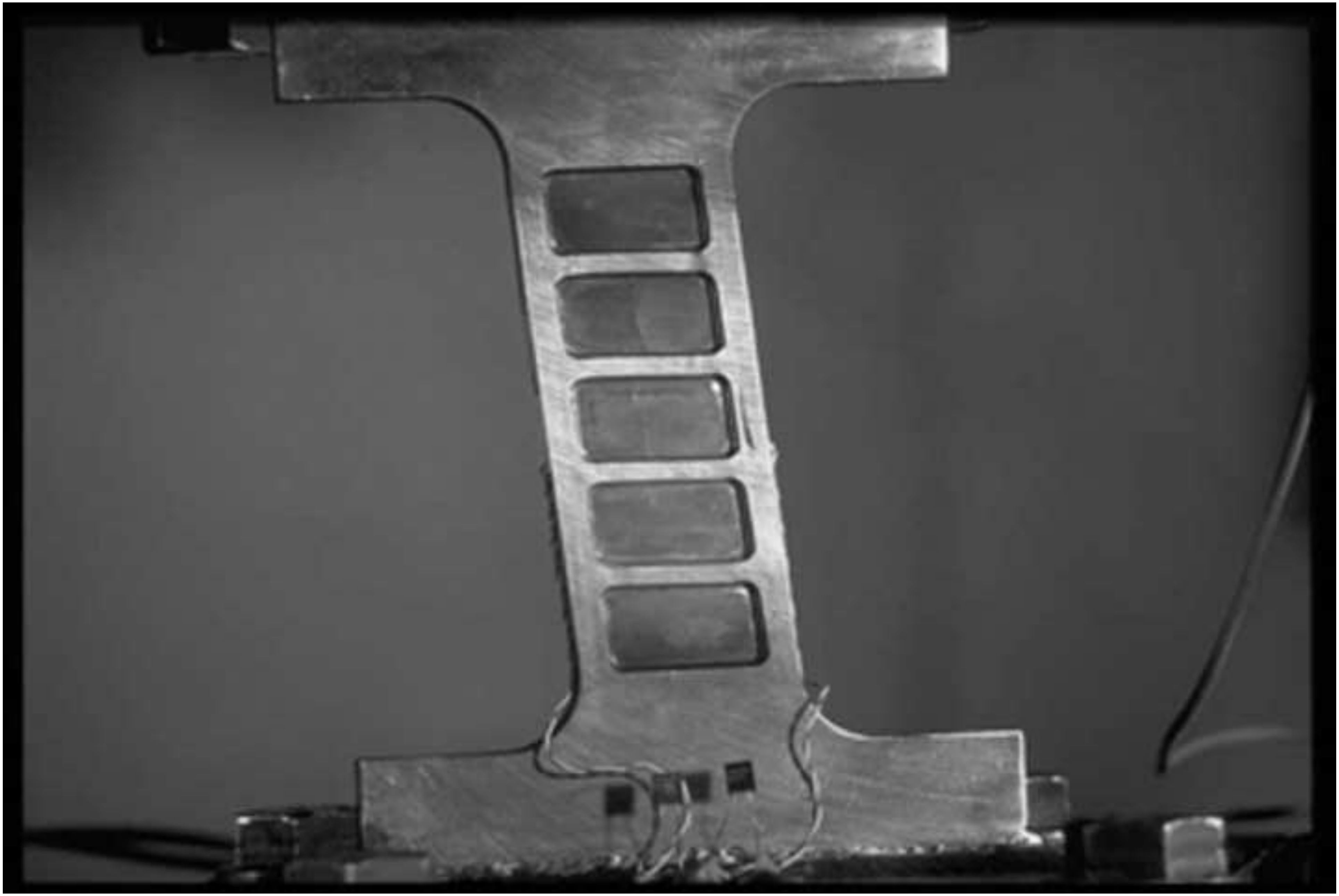

Figure 3b

Click here to download colour figure Fig. 3b.tif

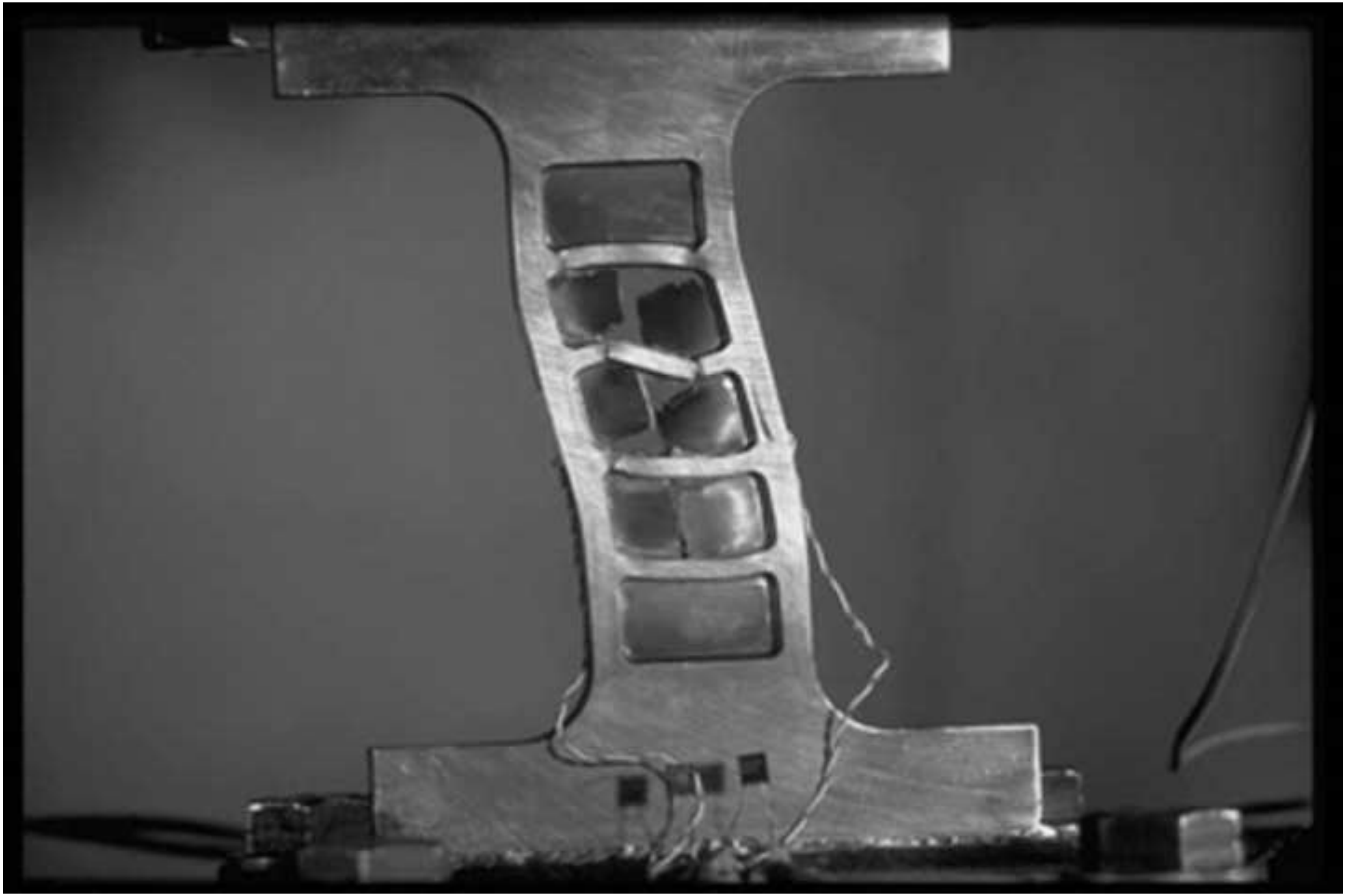

Figure 5

Click here to download colour figure Fig. 5.tif

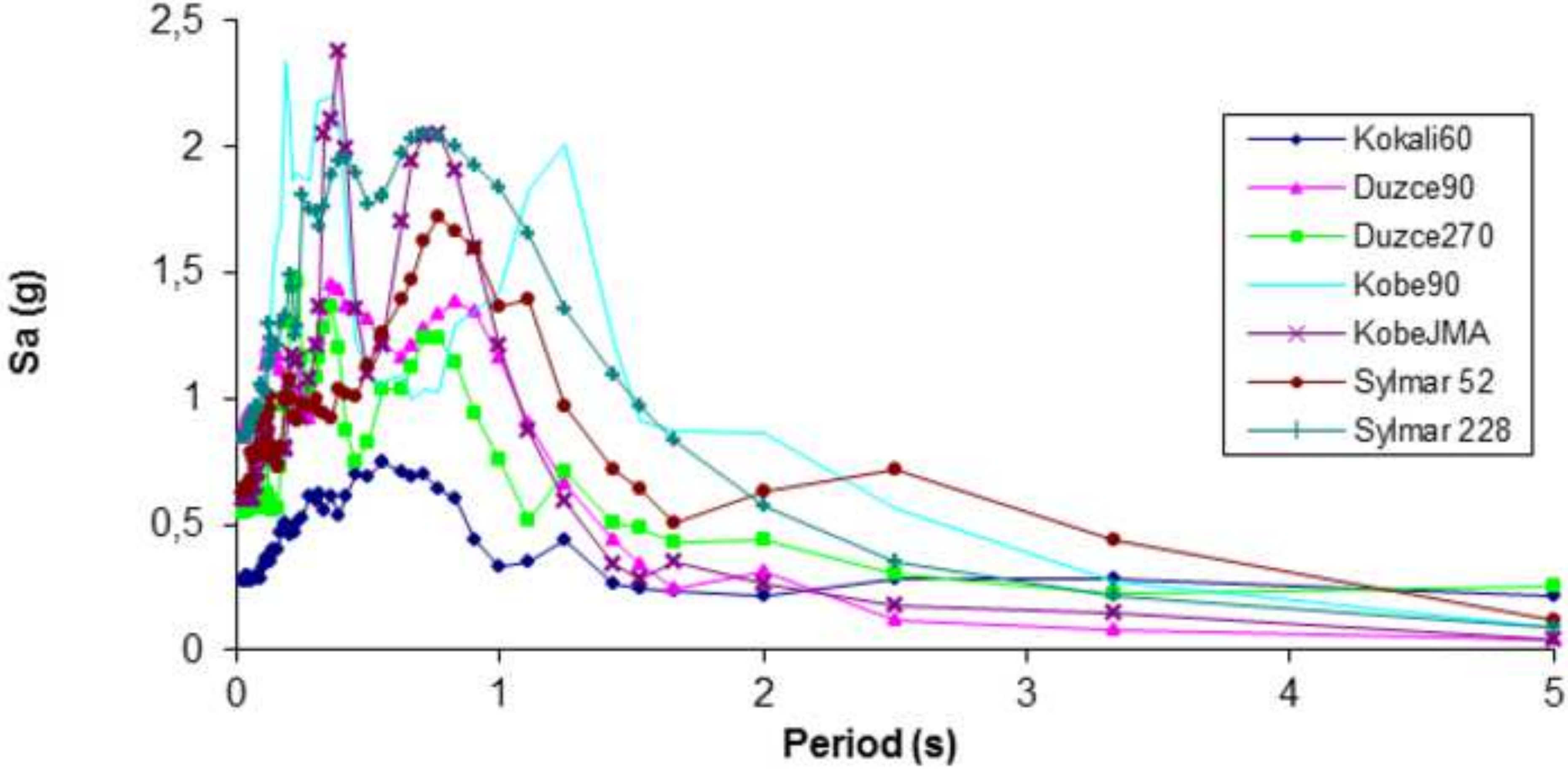

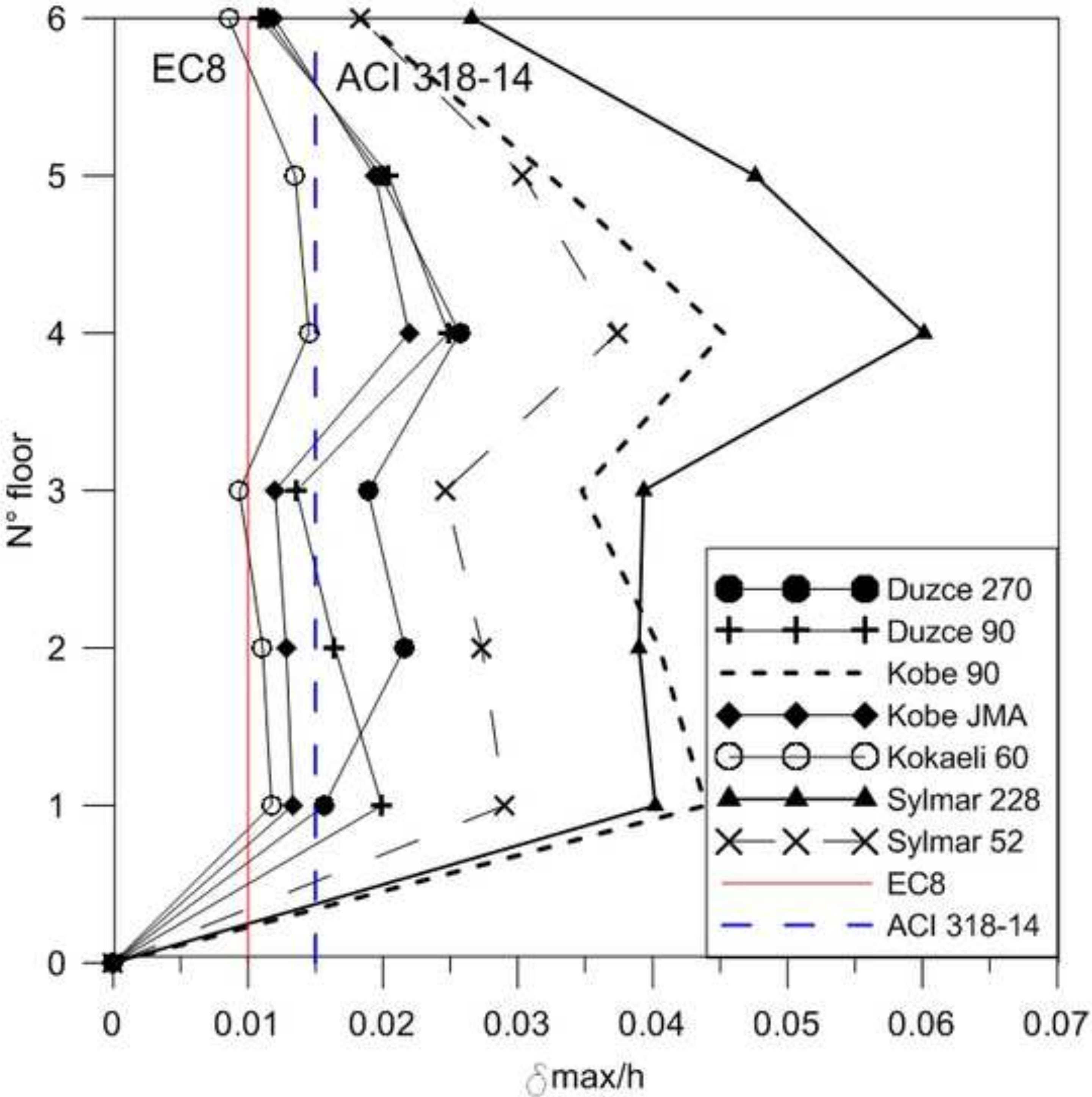

6
5
4
3
2
1
0
N° floor
EC8
ACI 318-14
0
0.01
0.02
0.03
0.04
0.05
0.06
0.07
δmax/h
Duzce 270
Duzce 90
Kobe 90
Kobe JMA
Kokaeli 60
Sylmar 228
Sylmar 52
EC8
ACI 318-14

Figure 6b Click here to download colour figure Fig.6B.jpg

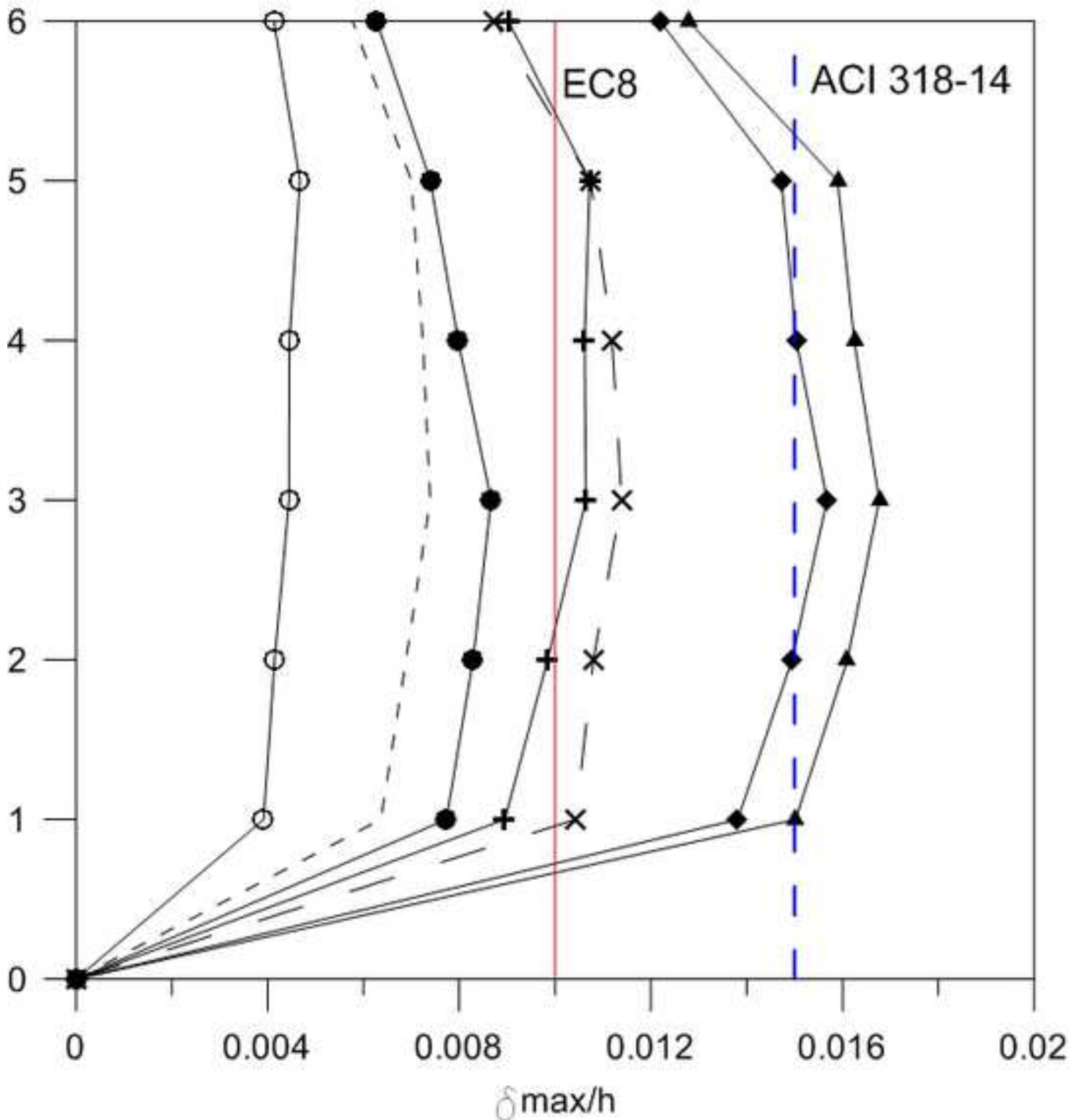

Figure 7a

Click here to download colour figure Fig.7A.jpg

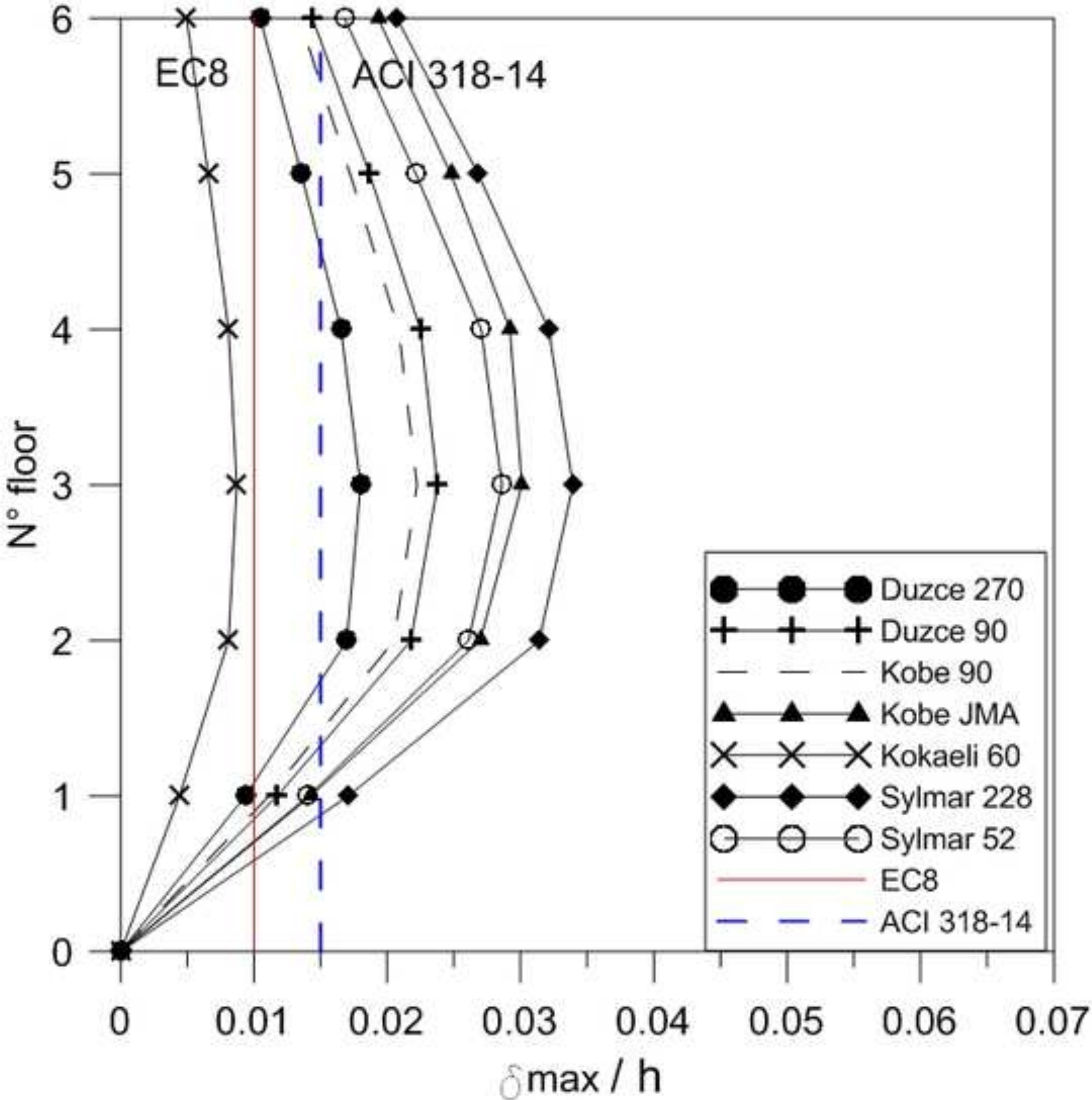

Figure 7b Click here to download colour figure Fig.7B.jpg

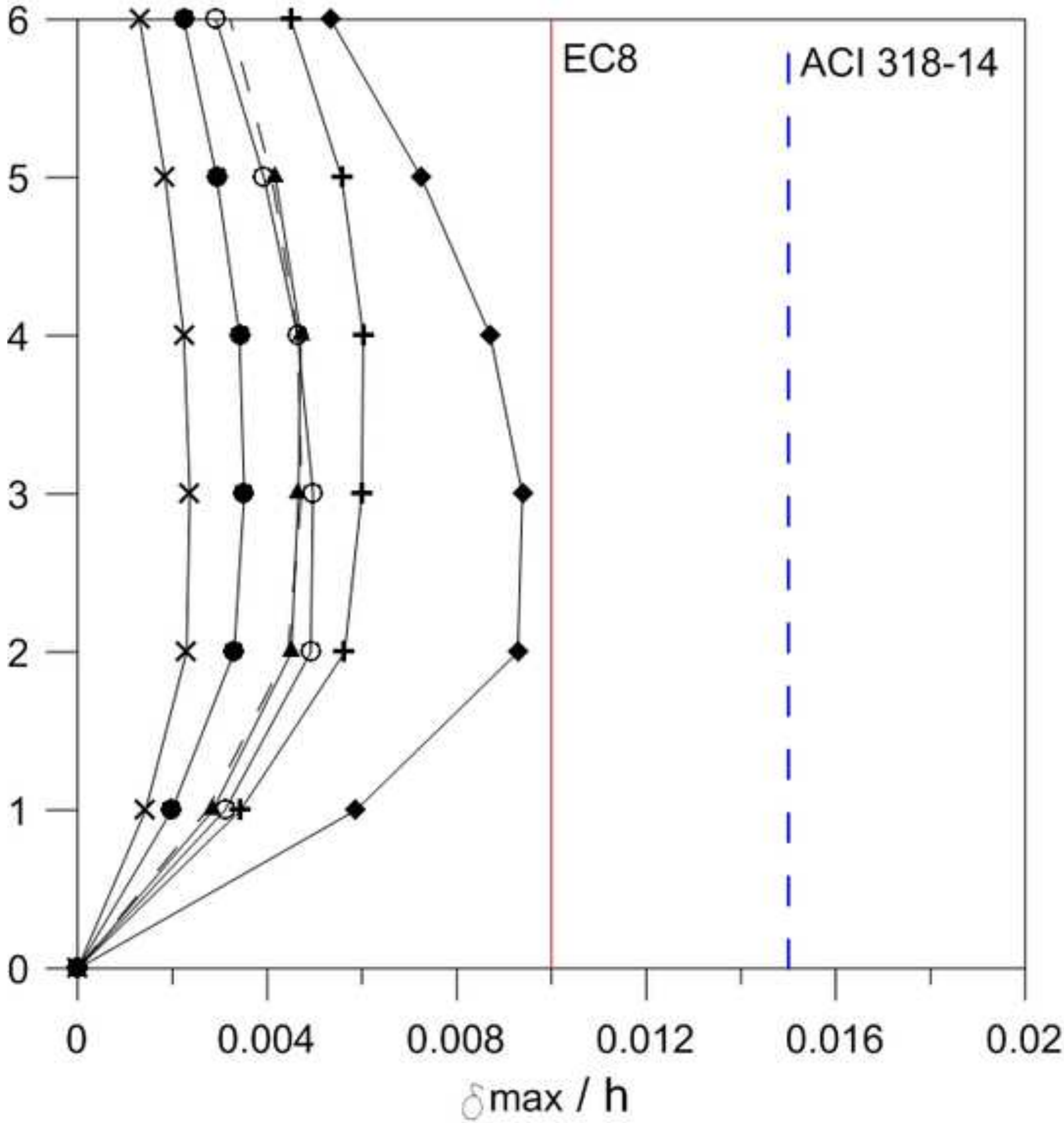

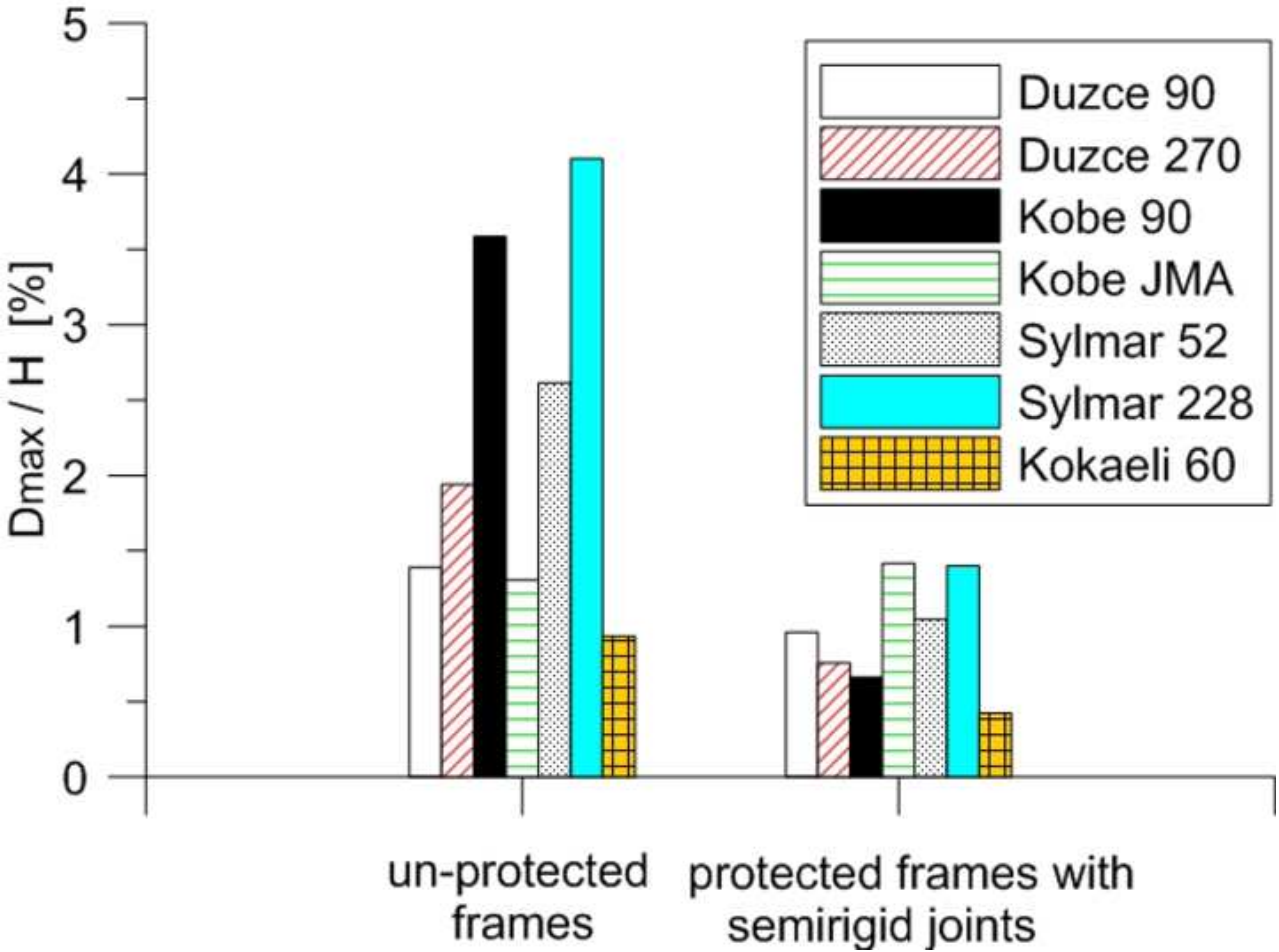
5
4
3
2
1
0
Dmax / H [%]
Duzce 90
Duzce 270
Kobe 90
Kobe JMA
Sylmar 52
Sylmar 228
Kokaeli 60
un-protected frames
protected frames with semirigid joints

Figure 8b

Click here to download colour figure Fig. 8b.jpg

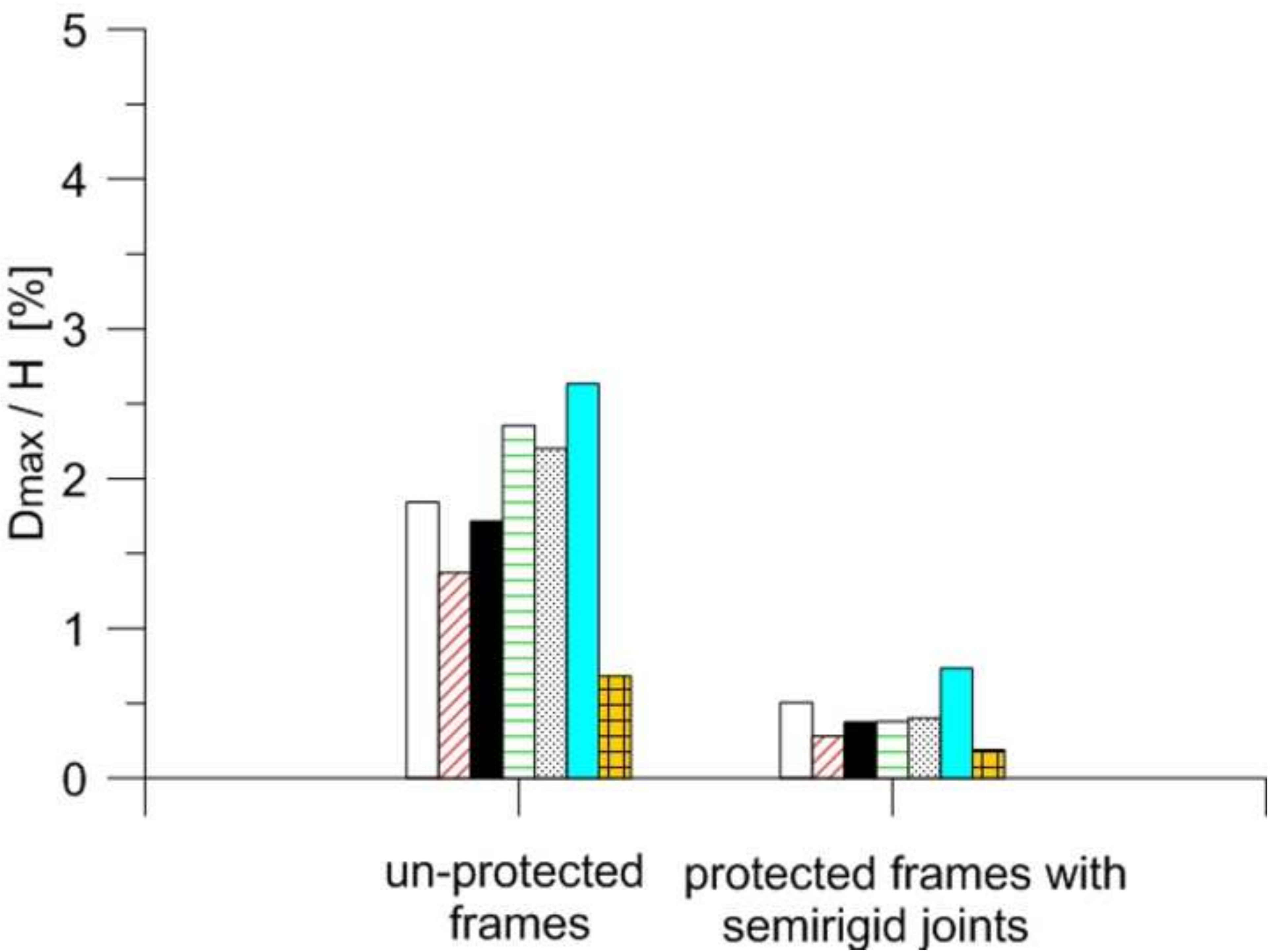

Figure 9a

Click here to download colour figure Fig. 9a.jpg

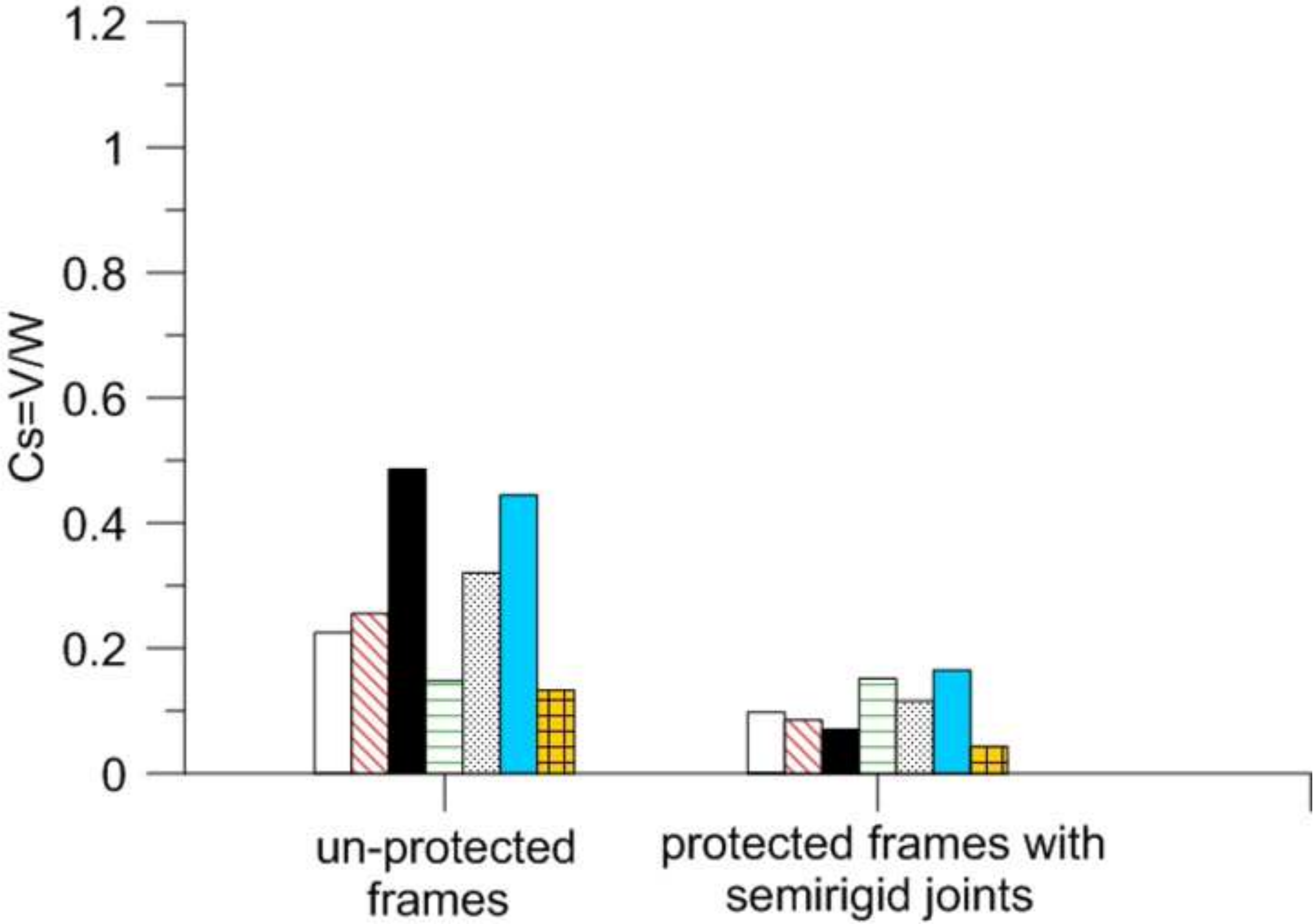

Figure 9b

Click here to download colour figure Fig. 9b.jpg

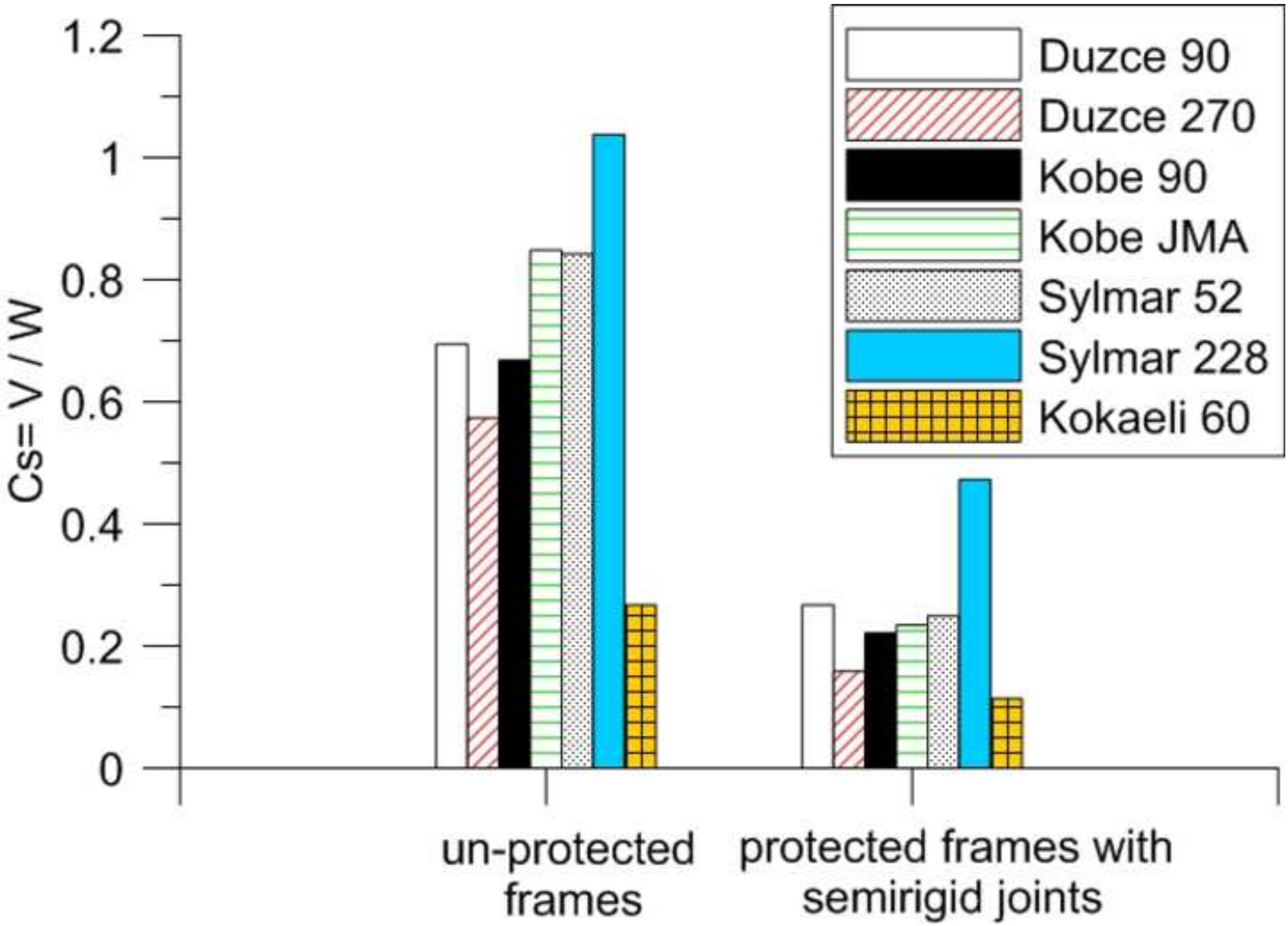

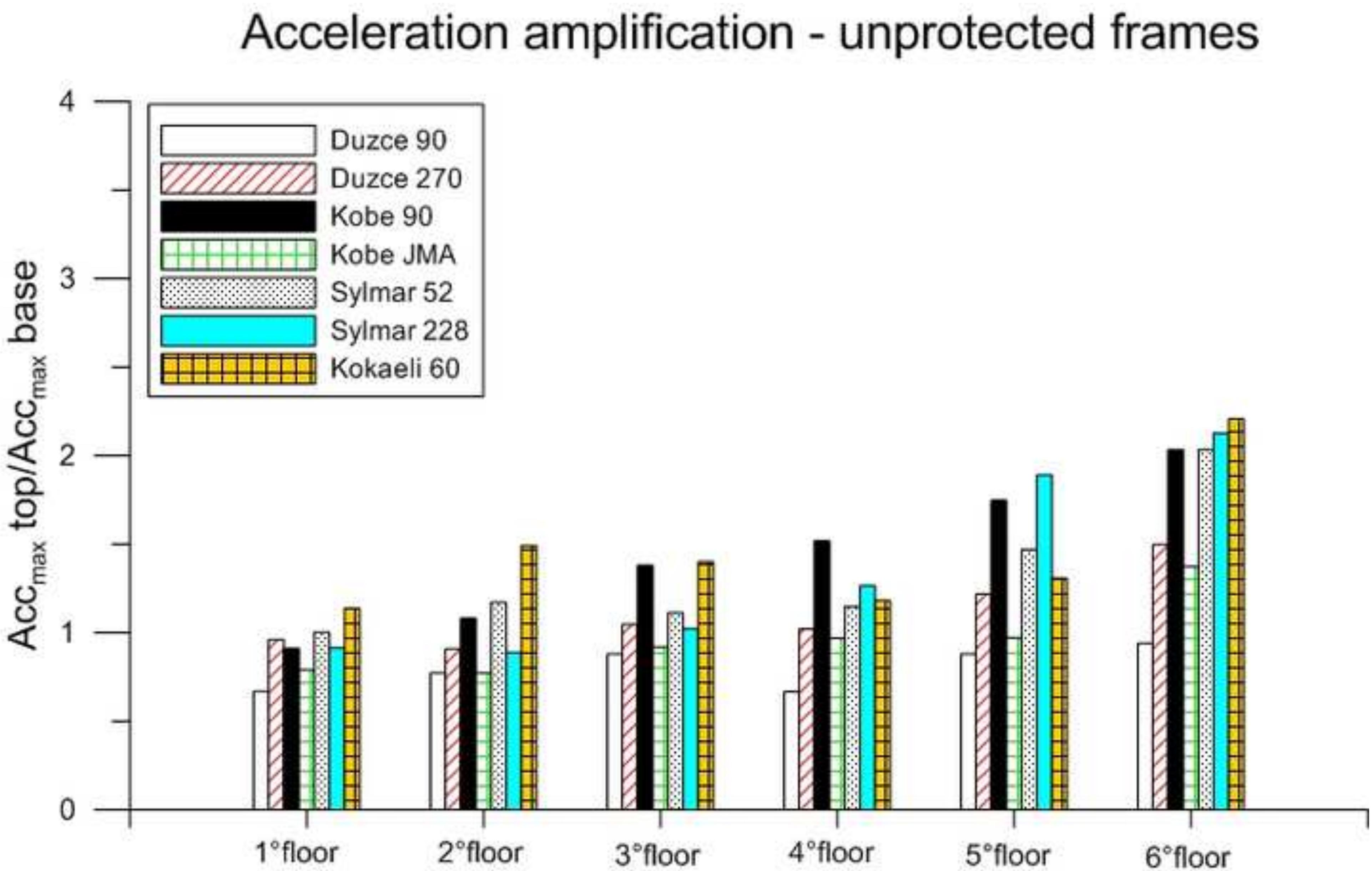
Acceleration amplification - unprotected frames
Acc_{max} top/Acc_{max} base
0
1
2
3
4
Duzce 90
Duzce 270
Kobe 90
Kobe JMA
Sylmar 52
Sylmar 228
Kokaeli 60
1°floor
2°floor
3°floor
4°floor
5°floor
6°floor

Figure 10b

Click here to download colour figure Fig.10B.jpg

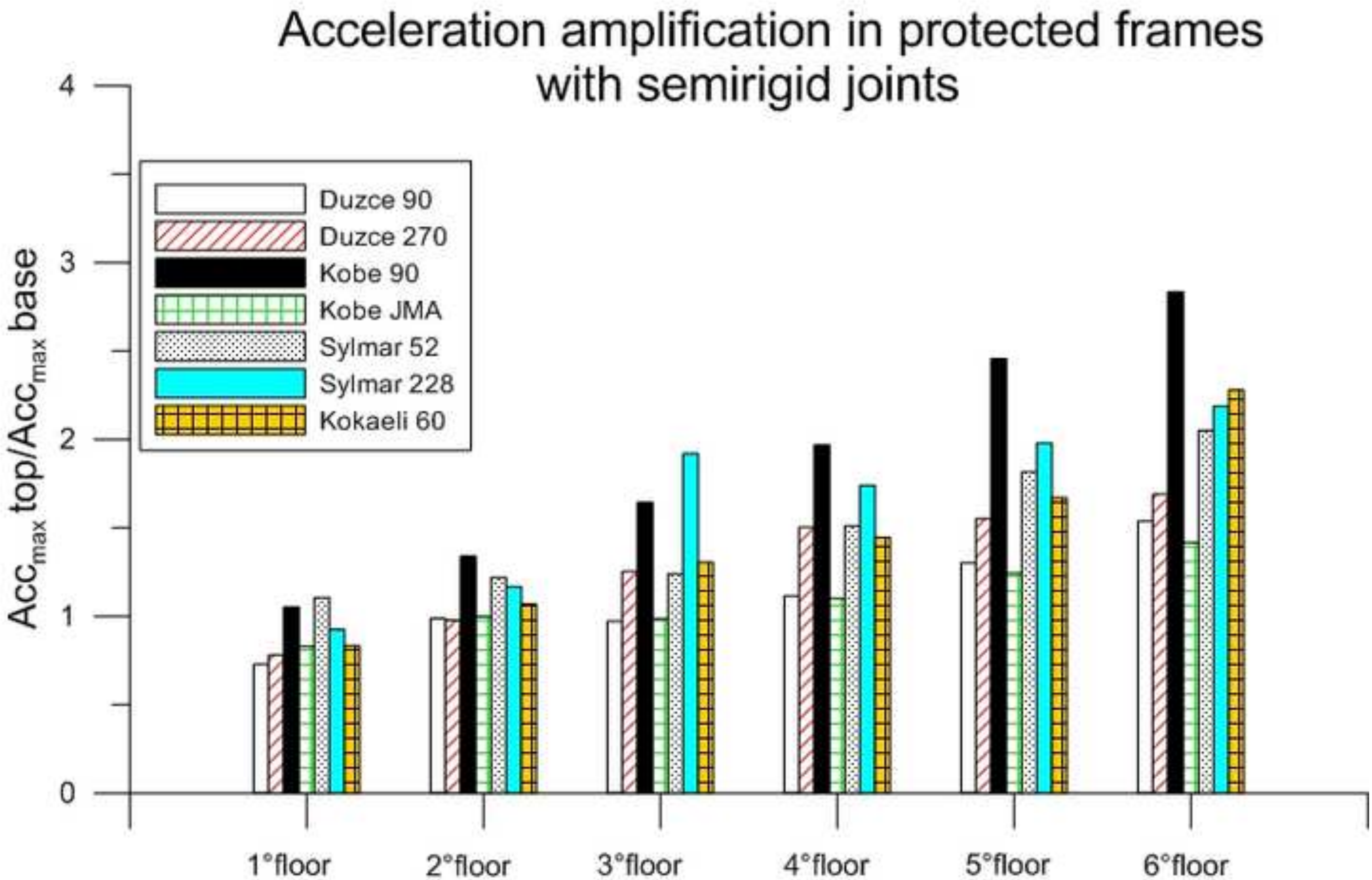

Figure 11

Click here to download colour figure Fig 11.jpg

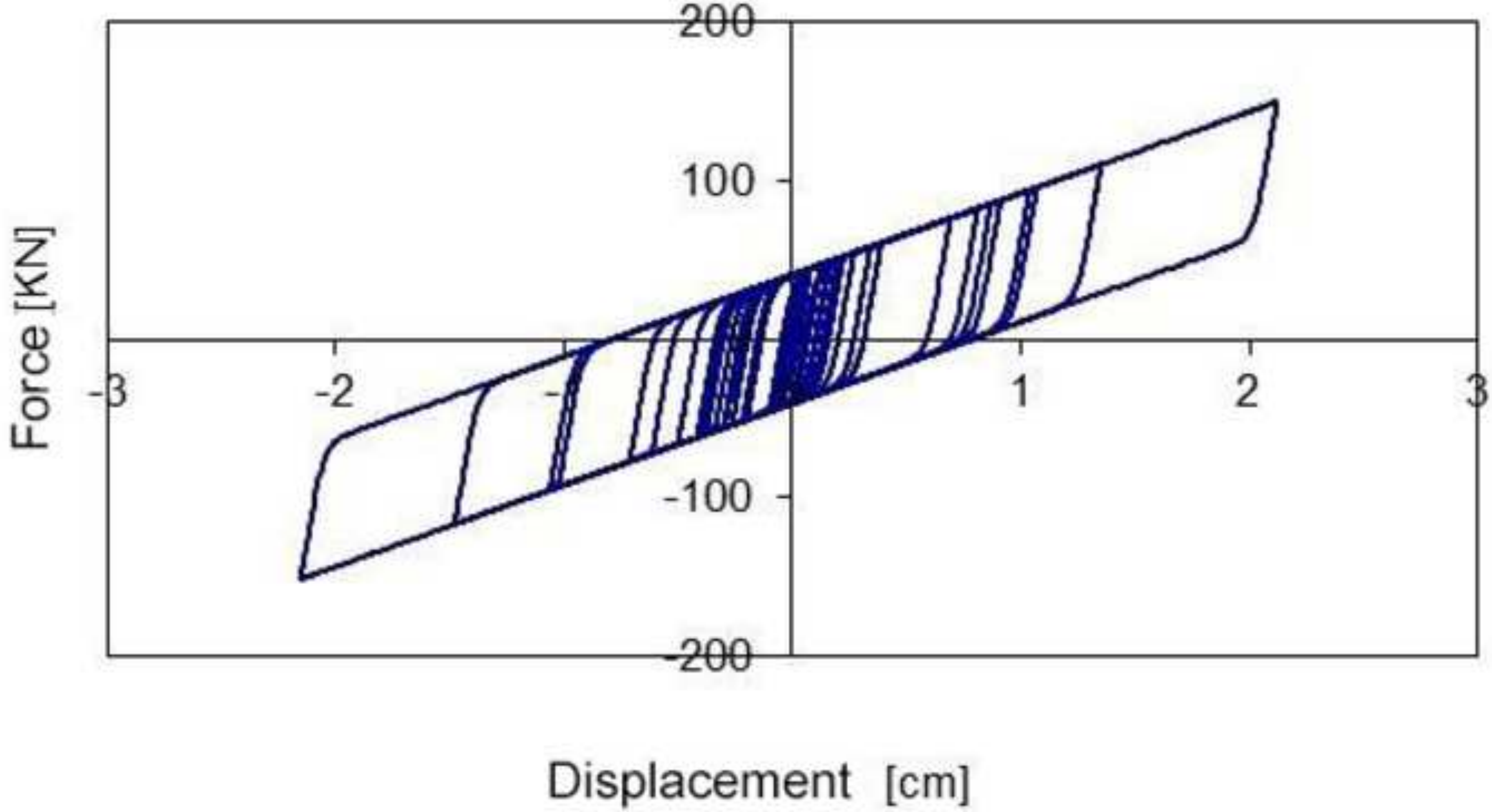

Figure 1

Click here to download line figure Fig. 1.jpg

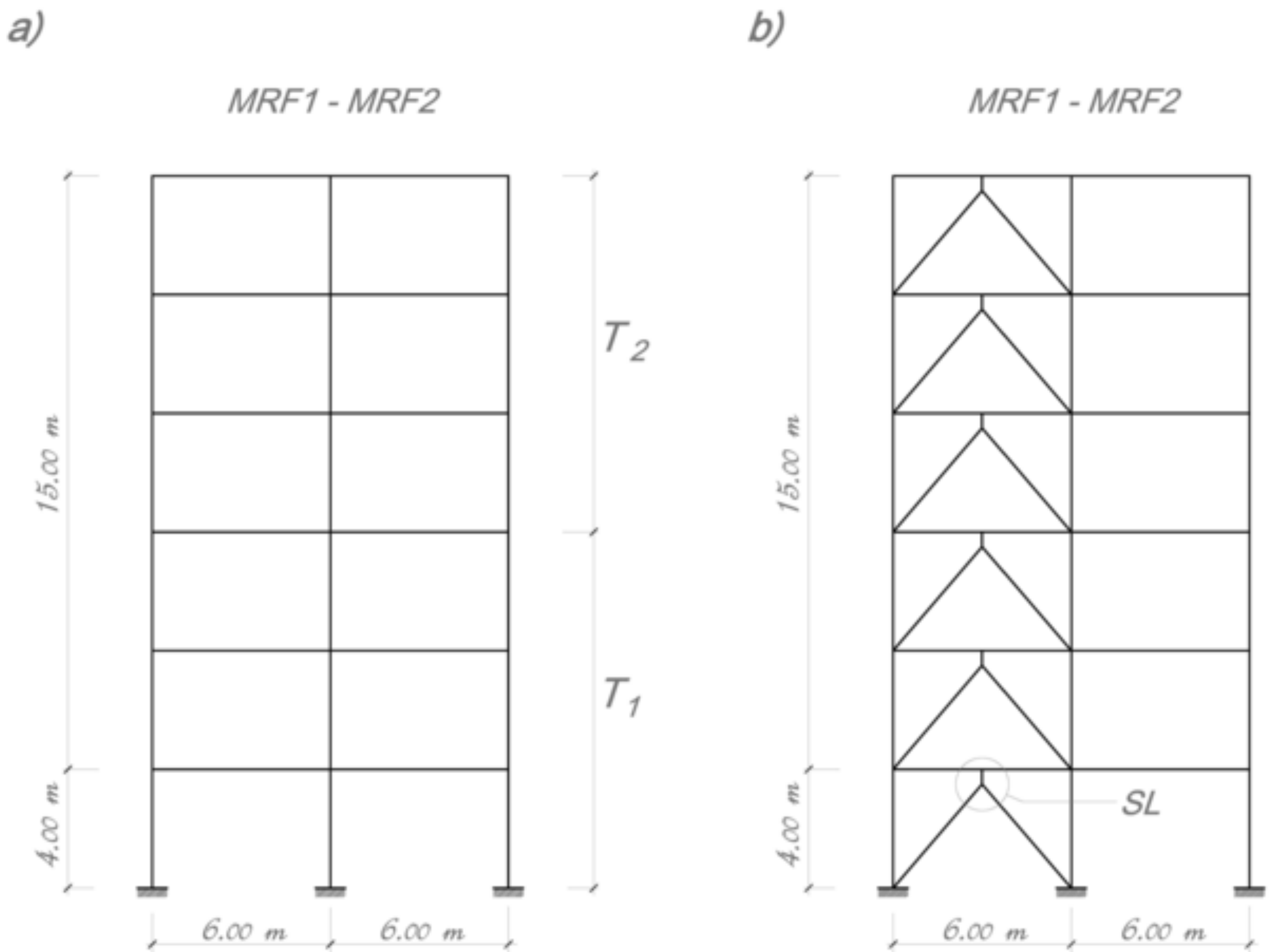

Figure 2a

Click here to download line figure Fig 2a.jpg

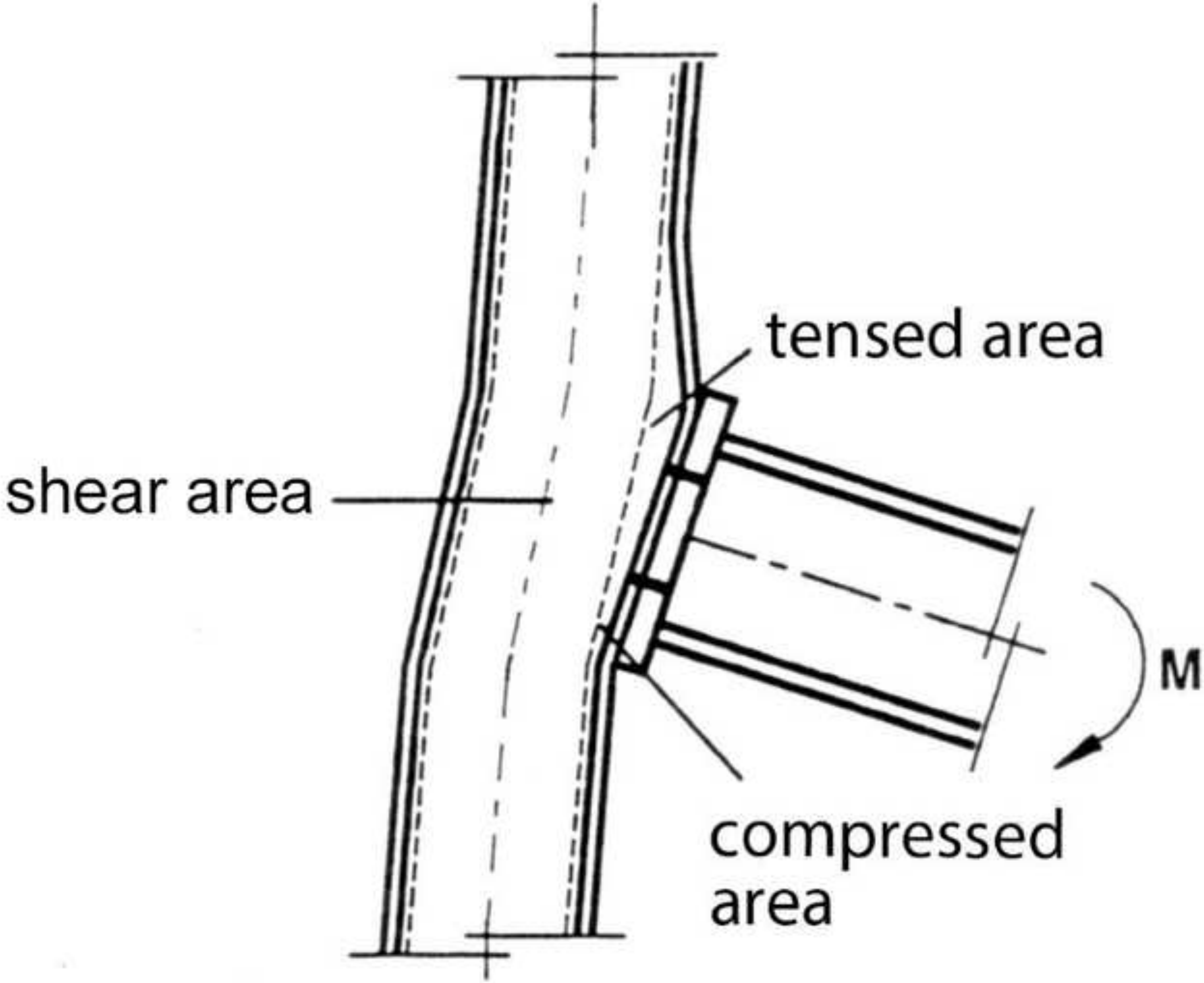

Figure 2b

Click here to download line figure FIG 2B.jpg

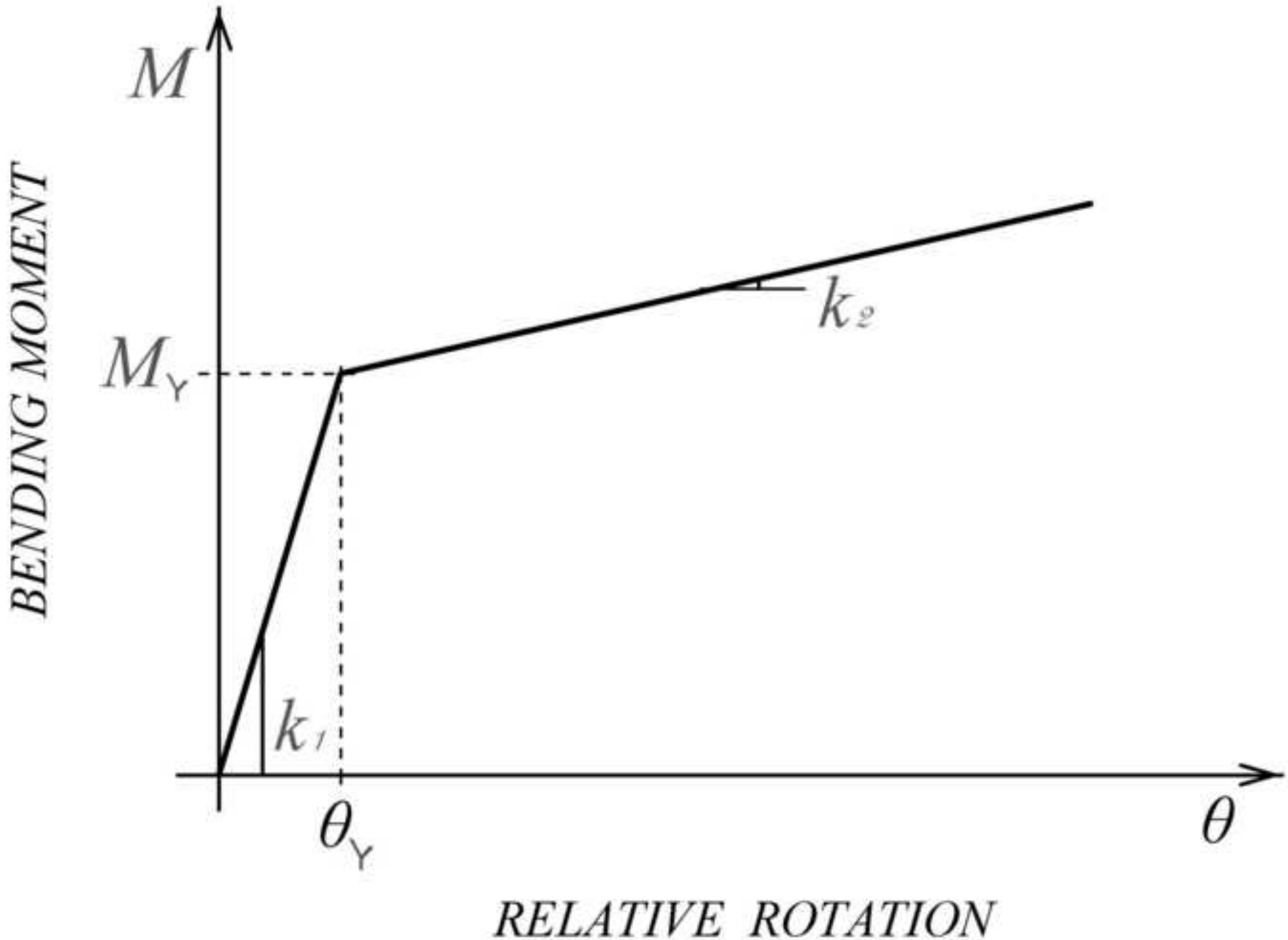

Figure 4

Click here to download line figure Fig. 4.tif